Structural analysis of unpaved reinforced roads

November 1998

R.G. Tjong-A-Hung

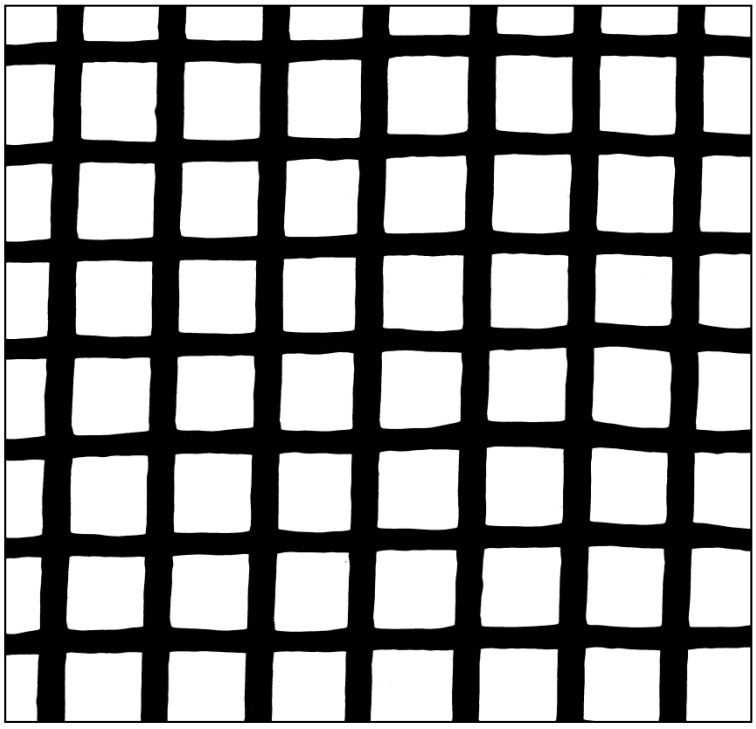

Table of contents

List of symbols and abbreviations

Table of Contents

1. Introduction and Scope

1.1 Introduction

Agriculture roads cover a big part of the total infrastructure. Characteristic for this kind of roads is that they usually have a very thin asphalt layer or no asphalt layer at all and that they are quite often built on a very weak subsoil, for example peat. These factors in combination with occasionally very high wheel loads will immediately lead to high stresses resulting in high displacements and early failure of the road structure.
One possible way of taking care of these problems is by means of road reinforcement. This can be done by applying a grid, a net or a woven interlayer (made of steel or synthetics) in the structure, especially at those areas where the tensile stress will dominate. In general the reinforcement is placed at the bottom of the base.
The reinforcement should be able to take these tensile stresses. This means that the stresses on the subsoil are lowered and the integrity of the structure will remain. The tensile forces in the structure are transmitted over to the grid by means of friction between aggregate and interface material.
There is no standard design method for the design of roads with reinforced bases. Therefore a theoretical analyses of roads with reinforced bases was made by means of the finite element program CAPA 2D. In this analysis the influence of various parameters was studied such as the stiffness of the subsoil as well as that of the base. Other parameters are the stiffness of the interface and of course the type of reinforcement and the applied load.
This stiffness of the interface is essential for the transmission of stresses in the reinforcement and can be divided in the normal stiffness (to avoid the reinforcement from sinking into the subsoil) and the lateral stiffness (for transmission of the horizontal stresses to the reinforcement)

1.2 Scope

The purpose of this report is to examine the behaviour of unsurfaced reinforced and unreinforced roads. This is done using the computer program BISAR and CAPA 2D.
In chapter 2 the problem is analyzed, defined, the preconditions are listed and expected results are given.
In chapter 3 the dimensions such as the thickness and the width of the road and the properties of the subsoil of the road are presented.
In chapter 4 one of the input parameters for CAPA 2D, the base stiffness is calculated. From this chapter it will be clear that the stiffness should be calculated in an iterative manner.
Chapter 5 discusses the parameters of influence for the calculations and some properties of CAPA 2D in general.
Chapter 6 gives the results of the calculations, assuming isotropic and partly isotropic behaviour.
In chapter 7 conclusions are presented and recommendations (for the next user(s)) are given.

2. Problem analysis

2.1 Definition of the problem

Agriculture roads often don't have an asphalt top layer and are regularly built on a very weak subsoil. In combination with occasionally very high wheel loads this will immediately lead to high stresses which result in high displacements and premature pavement failure. This can be minimized by introducing a reinforcement in the road structure. The question which remains is how does the road react to the reinforcement and what are the main parameters of influence.

2.2 Objective

The objective of this thesis is to present a possible way to design reinforced agriculture roads, taking the parameters of influence into account and/or at least give recommendations for the design.

2.3 Expected results

The following results are expected:

- The calculations will show that reinforcing has a positive influence on the behaviour of the structure.
- The calculations will be sensitive to the bond stiffness between the interface and the surrounding (aggregate) material (the higher the bond the better the forces can be transmitted into the grid thus the lower the displacements will be), the type of subsoil (the stiffer the subsoil, the lower the displacements), the thickness of the base (the thinner the base the bigger the displacements will be) and the stiffness of the base material.
- The difference for the displacements between reinforced and not reinforced pavement structures will be bigger when the base structure is less coherent and when cyclic loading is applied.
- Applying grids will be effective to a certain amount of stiffness. There is an optimal grid stiffness. A grid stiffness far below or above the optimal stiffness will have hardly any effect on the displacements of the pavement structure.

2.4 Limitations

The analyses are limited with some preconditions and starting points. They are presented hereunder:

2.4.1 Preconditions

The preconditions for the analyses are:

- The calculations are linear elastic.
- The load is considered to be static.
- The load is considered to be a distributed load.
- The material is homogeneous.
- The finite element calculations with CAPA are done 2 dimensionally.

- The load will follow only one wheel track (channelized traffic).
- The dead weight of the pavement structure is excluded in the finite element analysis with CAPA (one is only interested in the behaviour due to the applied wheel loads).

2.4.2 Starting points

The starting points for the analyses are:

- Because of symmetry only half the road is considered.
- The total width of the road is 4.5 meter.
- The load has a contact pressure of 0.707 MPa.
- The base can bear some tension due to the (very high) cohesion.

3. Dimensions and Properties

In this chapter an outline of the soil properties and dimensions of the structure to be analyzed are presented.

3.1 Dimensions

3.1.1 Width of the road

In figure 3.1 an outline of a typical rural road is shown. The width of the road is 4.5 meters. On both sides of the road there are ditches. This means that the sides are able to move freely in x-direction as well as in y-direction to a certain depth. Below this depth the structure goes to infinity. This goes for the x as well for the y direction.

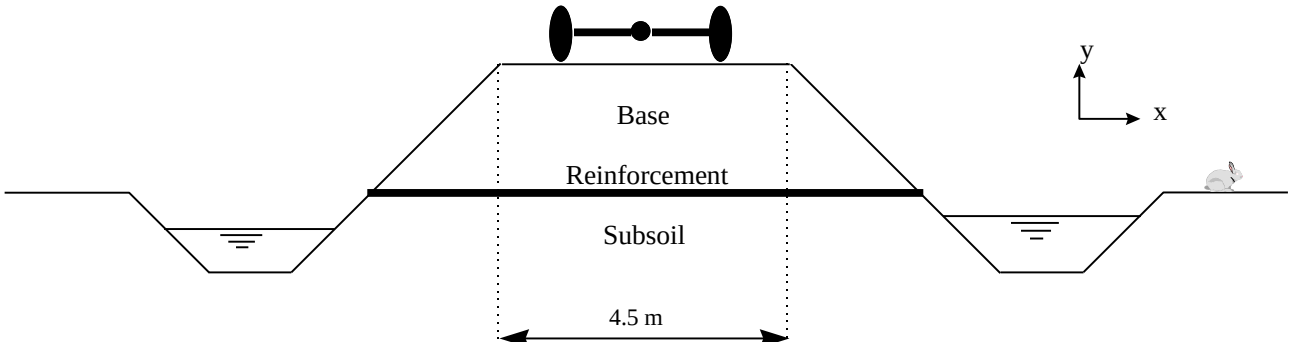

Figure 3.1 Exaggerated outline of a rural road

3.1.2 Base thickness

For the thickness of the base three different values are considered.
A thin base of 200 mm, a medium base of 350 mm and a thick one of 500 mm.
The base will be divided in different sublayers in order to simulate stress dependent behaviour of the unbound base material.
The 350 mm and 500 mm thick base are both divided in 4 sublayers. The 200 mm thick base isn't divided in 4 sublayers but in 5 sublayers, this is done because determination of the base stiffness (chapter 4) with 4 sublayers won't provide satisfying stiffnesses due to the relatively thin base.

For the thickness of the sublayers see table 3.1.

Base thickness (mm)	Thickness of each base sublayer (mm)				
500	125	125	125	125	-
350	100	100	75	75	-
200	100	25	25	25	25

Table 3.1 Division of the base into different sublayers

In figure 3.2 the division is visualized for the 500 mm thick base.

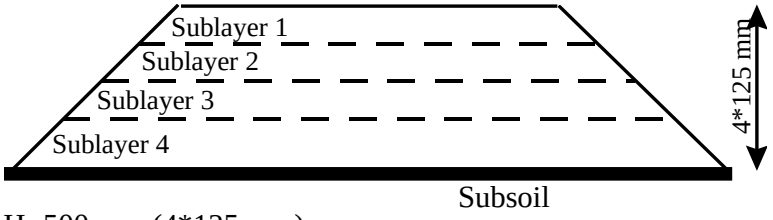

H=500 mm (4*125 mm)

Figure 3.2 The sublayers for the 500 mm base

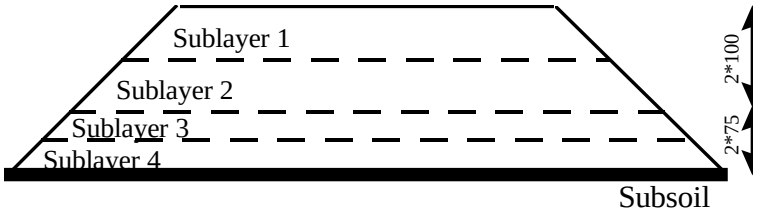

H=350 mm (2*75+2*100 mm)

Figure 3.3 The sublayers for the 350 mm base.

In Figure 3.3 this is done for the 350 mm base and in figure 3.4 this is done for the 200 mm base.

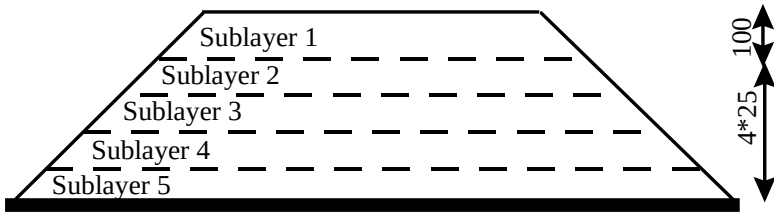

H=200 mm (4*25)

Figure 3.4 The sublayers for the 200 mm base

3.2 General properties

3.2.1 The subsoil

In the analyses the subsoil is assumed to be a very weak clay or peat. The consequence of this is that the structure will deform extensively and failure will possibly occur. To prevent this phenomenon the structure can be reinforced with e.g. a geotextile.
Geotextiles can be applied for this kind of roads which are built on a clay or a peat subsoil as mentioned above.

To show the difference in the behaviour of the road in relation to the type of subsoil, the following stiffness values are assumed:

1. Very weak peat (Dynamic E-modulus of 10 MPa)
2. Normal peat or weak clay (Dynamic E-modulus of 25 MPa)
3. Normal Clay (Dynamic E-modulus of 50 MPa)

3.2.2 The base material

The base material used is a mixed granulate. A mix granulate consists of concrete- and masonry rubble.

Some properties for the base material are[1]:

- Resilient modulus $M_r = k_1\ \theta^{k2}$ with k_1=34 MPa; k_2=0.38 and θ the sum of the principle stresses (also see chapter 4).
- cohesion c = 70 kPa ; angle of internal friction $\phi = 55^0$

The factors k_1 and k_2 are needed as input parameter for the stress dependent determination of the elastic moduli (see chapter 4 for these calculations). The factor c is the cohesion (kPa), the high value indicates that the material is lightly bounded. The factor ϕ is the angle of internal friction (in degrees) of the aggregate.

3.2.3 Specifications of the load

The applied wheel load for the BISAR and the KENLAYER calculations (both 3 dimensional, see chapter 4) is 50 kN. With a contact area with a diameter of 300 mm the load can be simulated by a distributed vertical load with a contact pressure of 0.707 MPa, see figure 3.2. The distance between the wheels is 2.3 m.

For the finite element calculations with CAPA (2 dimensional) a distributed line load with a contact pressure of 0.707 MPa is applied (see chapter 6).

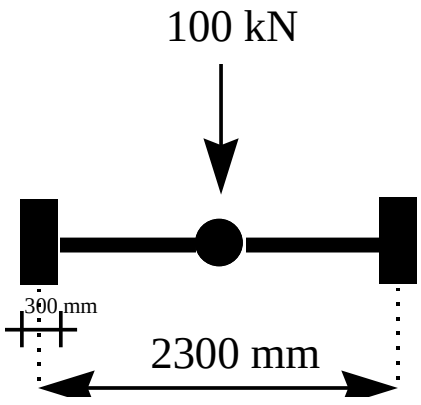

Figure 3.5 Outline of the wheel

When it appears that the load of 50 kN can't be carried by the structure, a lower value will be used instead. In chapter 4 it will be clear that the 50 kN load is indeed too big.

[1] These values are obtained from the report "Survey base materials test sites Schipluiden" by H.E.W. Jansma and ir. G.T.H. Sweere, june 1988

4. Determination of the base stiffness

One important input parameter for the CAPA calculations is the Young's modulus of the base material. There are different manners of determining this modulus. In this chapter some attempts to calculate this modulus are presented.
In paragraph 4.1 and 4.2 the first attempts are presented and reasons are given why the output of them is useless. In paragraph 4.3 the final way to obtain the base stiffness is described.

The three attempts to determine the stiffness are:

1. Kenlayer.
2. M_r-σ_3–σ_1 iterations.
3. Bisar iterations considering failure.

4.1 Kenlayer

Kenlayer is a linear-elastic program which can be applied to multi-layered systems under various types of loading (single, dual dual-tandem or dual-tridem) with each layer behaving differently.
With Kenlayer it is possible to compute principle stresses, strains and displacements of a multi-layered system under a circular load. It is also possible to perform damage analyses for fatigue cracking and permanent deformation.
Here Kenlayer is used to determine the stress dependent stiffness of the base. The program uses the M_r-θ material model. This model is schematically given by figure 4.1. The figure shows that when the vertical stress increases, the stress invariant θ ($\theta = \sigma_1+\sigma_2+\sigma_3$) will also increase and by consequence also the resilient modulus M_r will increase.

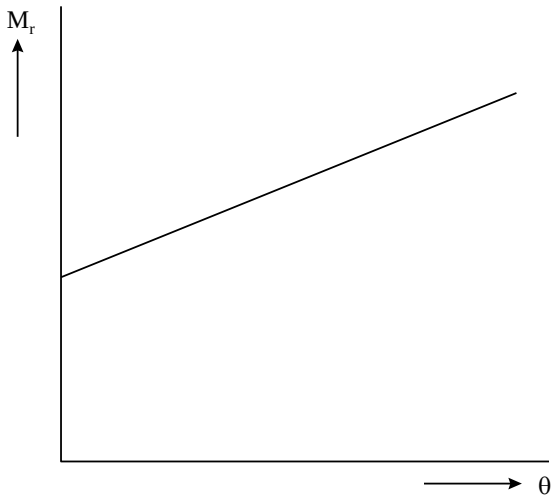

Figure 4.1 M_r-θ material model

The basic calculation procedure for the stress dependent stiffness (resilient modulus) is:

- Division of the base into a number of sub-layers
- Calculation of the stresses at the mid-depth of each layer
- Calculation of the resilient modulus with the M_r-θ material model.

4.1.1 Input Kenlayer

The main input parameters are:

- The load;
  The load is a 50 kN wheel load on a circular area with a radius of 150 mm, leading to a contact pressure of 0.707 MPa.

- Material parameters;
  k_1=34 MPa and k_2=0.38.

- The maximum stiffness;
  The maximum elastic modulus is initially computed using:
  The vertical stress on top of the base σ_v, 0.707 MPa.
  1. An estimation of the horizontal stress (10% of σ_v), 0.0707 MPa.

  This gives a maximum modulus on top of the base of 440 MPa using the M_r-θ relationship.

- All interfaces between the sublayers are fully bonded.

- The calculation points;
  In the middle of each sublayer.
  (in the case of a 500 mm thick base this will be at 62.5, 187.5, 312.5 and 437.5 mm).

- The stiffness of the subsoil (10, 25 and 50 MPa).

- The unit weight of the base (18 kN/m^3).

4.1.2 Output Kenlayer

Table 4.1 gives the output for the stresses for the 500 mm base on a 10 MPa stiff subsoil computed by Kenlayer. Table 4.2 shows the used stresses to compute the resilient modulus. In annex 2.1 the total Kenlayer output is shown.

Computed Stresses in sublayers (kPa)				
	Sublayer 1	Sublayer 2	Sublayer 3	Sublayer 4
σ_1	624	272	94.9	27.8
σ_2	386	-29.9	-79.8	-93.7
σ_3	386	-29.9	-79.8	-93.7

Table 4.1 Stresses in sublayers

Final stresses used to compute Elastic modulus (kPa)				
	Sublayer 1	Sublayer 2	Sublayer 3	Sublayer 4
σ_1	625	276	101	35.7
σ_2	387	0	0	0
σ_3	387	0	0	0

Table 4.2 Stresses used to compute M_r including geostatic stresses

Table 4.3 shows the computed stiffnesses. From the output it is concluded that the computed moduli are very high.

Elastic moduli of the 500 mm base (MPa)				
Sublayer 1	Sublayer 2	Sublayer 3	Sublayer 4	Subsoil
533	290	198	133	10

Table 4.3 Computed elastic moduli with Kenlayer (rounded)

From the output of Kenlayer (table 4.1) it can be seen that some of the sublayers are in tension. This can occur to a certain level due to the cohesion of the mix granulate.

The program Kenlayer has as starting point that occurrence of tension is impossible. Because of this Kenlayer sets the stresses of the layers in tension to zero (see table 4.2). The consequence of this is that the computed moduli will be rather high because the stress invariant (θ) is bigger compared with the tension case. The output could therefore be less realistic and another approach must be used to determine the moduli.

For the second sublayer an illustration of this is given hereunder:

For the tension case this would lead to a M_r of (for the data see table 4.1):

$\theta=\sigma_1+\sigma_2+\sigma_3+3*\sigma_{dw}$=> 272-(2*29.9) + (3*3.375) = 222 kPa

$M_r=34 \cdot 222^{0.38}$ = 265 MPa.

For the case where the tension is omitted this gives (see table 4.2 for the data):

$\theta=\sigma_1+\sigma_2+\sigma_3+3*\sigma_{dw}$ => 276+0+0+ (3*3.375) = 286 kPa.

$M_r=34 \cdot 286^{0.38}$ = 290 MPa.

The difference between the two cases is for the second sublayer 25 MPa. For the other sublayers this difference is even bigger due to the higher horizontal tensile stresses.

4.2 M_r-σ_3–σ_1 iterations

As described in the previous section, a possible manner to determine the elastic modulus of the base structure is by using the M_r-θ material model. The M_r-θ model has as disadvantage that when the vertical stress increases, θ will also increase and by consequence also M_r will increase (see figure 4.1). Of course, this isn't possible, at a certain point a further increase of the vertical stress should lead to failure.
The M_r-σ_3–σ_1 model prevents this to occur. In figure 4.2 one can see that for a constant level of σ_{conf} M_r decreases if the value of σ_1 (thus θ) increases. The figure shows furthermore that an increase of σ_{conf} leads to an increase of M_r.
The M_r-σ_3–σ_1 model is capable to describe this phenomenon, in contrast to the M_r-θ model.

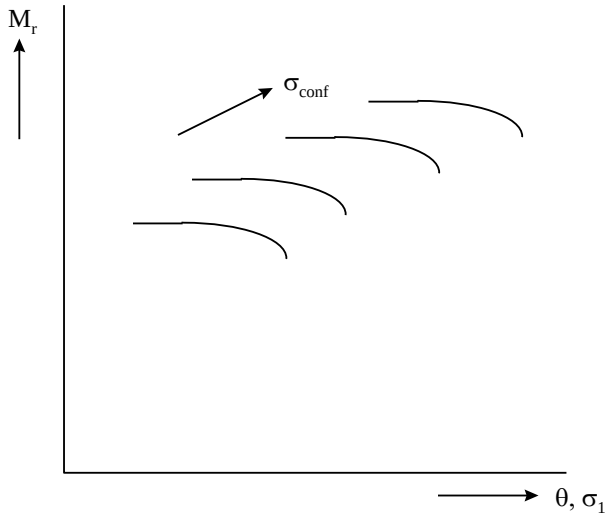

Figure 4.2 M_r-σ_3–σ_1 model

The M_r-σ_3-σ_1 model is given by equation 4.1:

$$M_r = k_5 \left[\frac{\sigma_{conf}}{\sigma_0} \right]^{k6} \cdot \left[1 - k_7 \left[\frac{\sigma_1}{\sigma_{1,f}} \right]^{k8} \right] \tag{4.1}$$

where:

$\sigma_{1,f}$	: σ_1 at failure according to Mohr-Coulomb $= \frac{(1+\sin\phi)\cdot\sigma_{conf} + 2c\cdot\cos\phi}{1-\sin\phi}$	(kPa) (4.2)
c	: cohesion	(kPa)
ϕ	: angle of internal friction	(^{0})
σ_{conf}	: confining pressure	(kPa)
k5	: model parameter	(MPa)
k6,k7,k8	: model parameter	(-)
σ_o	: reference stress	(1 kPa)

The first term of equation 4.1 can be compared with the M_r-θ model, the second term describes the decreasing effect on M_r with increasing σ_1.

The iteration process will be executed by making use of the M_r-σ_3–σ_1 model.

At first an outline of the followed procedure is described hereunder:

Step 1
The used moduli for the first iteration step are obtained from the program Kenlayer (table 4.3).

Step2
The equivalent layer thickness is calculated using Odemark's equivalency theory:

$$H_{eq}=0.9*H_{base}\sqrt[3]{\frac{E_{base}}{E_{subsoil}}} \tag{4.3}$$

Step 3
Compute the vertical stress due to traffic with Boussinesq's equation:

$$\sigma_z = q\left[1 - \frac{z^3}{(a^2 + z^2)^{1.5}}\right] \tag{4.4}$$

Step 4
Compute the horizontal stress due to traffic also with Boussinesq's equation:

$$\sigma_{x,y} = \frac{q}{2}\left[1 + 2\nu - \frac{2(1+\nu)z}{(a^2 + z^2)^{0.5}} + \frac{z^3}{(a^2 + z^2)^{1.5}}\right] \tag{4.5}$$

with

z	: depth	(mm)
a	: radius of the loaded area	(mm)
μ	: poisson's ratio	(-)
σ_z	: vertical stress at equivalent depth z	(kPa)
$\sigma_{x,y}$	: horizontal stress at equivalent depth z	(kPa)

Step 5
Compute the vertical and horizontal stresses due to the deadweight with:

$$\sigma_{vw} = h_{subl} * \rho_{base} \tag{4.6}$$

$$\sigma_{hw} = K_0 * \sigma_{vw}$$

with $K_0 = 1 - \sin \phi$

where

σ_{vw}	: vertical stress due to the dead weight	(kPa)
σ_{hw}:	: horizontal stress due to dead weight	(kPa)
h	: considered thickness	(mm)
ρ_{base}	: volumetric weight of the base	(kPa/mm)
K_0	: lateral stress ratio	(-)

The coefficient K_0 is assumed to be 1, due to compaction and for reasons of simplicity.

Step 6
Compute the resilient modulus according to (4.1):

$$M_r = k_5\left[\frac{\sigma_{conf}}{\sigma_0}\right]^{k6} \cdot \left[1 - k_7\left[\frac{\sigma_1}{\sigma_{1,f}}\right]^{k8}\right]$$

The model parameters in the model are[2]:

k5 = 120 MPa; k6 = 0.36; k7 = 0.191; k8 = 8.626.

Step 6
Go back to step 1 using the new resilient modulus, until the difference is 1%.

4.2.1 Iterations

The initial Young's modulus needed for the first iteration step is obtained from Kenlayer (paragraph 4.1.2, table 4.3).
The six steps described in paragraph 4.2 are integrated in a spreadsheet.

4.2.2 Output

In table 4.4 the last iteration step for the vertical and horizontal stresses due to traffic and stresses due to the dead weight are shown. The complete output (all the iteration steps) is shown in annex 2.2.

Output stresses due to traffic and dead weight (kPa)			
	σ_{vert}	σ_{hor}	σ_{dw}
Sublayer 1	365	23	1.1
Sublayer 2	84	-2.6	3.4
Sublayer 3	37	-1.6	5.6
Sublayer 4	19	-0.9	7.9

Table 4.4 Output stresses last step M_r-σ_3-σ_1 iterations

Table 4.5 shows the finally used stresses to compute the resilient modulus.

Output Iterations (kPa)					
	σ_{conf}	$\sigma_{1,f}$	σ_1	$k_7 (\sigma_1/\sigma_{1,f})^{k8}$	M_r
Sublayer 1	24	684	366	$-8*10^{-4}$	376
Sublayer 2	0.78	452	88	$-1*10^{-7}$	110
Sublayer 3	4.1	485	43	$-1*10^{-10}$	199
Sublayer 4	7.0	514	27	$-1*10^{-12}$	242

Table 4.5 Output last step M_r-σ_3-σ_1 iterations

The course of the resilient modulus is curious. The second term of formula 4.1 is almost 1 (due to the very small values of column 5, see table 4.5).
This means that the second term has hardly any influence on the stiffnesses. The resilient modulus is therefor only dependent on σ_{conf}, of which the development (and thus M_r) is shown in figure 4.3.
The values for the resilient moduli are plausible, according to the material properties (this is because of the high value for k_5 = 120 MPa).

[2] These values are Obtained from "The strength- and stiffness development of hydraulic mixed granulate" by P.J. van Beers, June 1998.

When using a linear elastic computer program such as Bisar with the stiffnesses of table 4.5 as input values, the computed horizontal stresses at the bottom of the base will immediately lead to failure, because of the high tension.

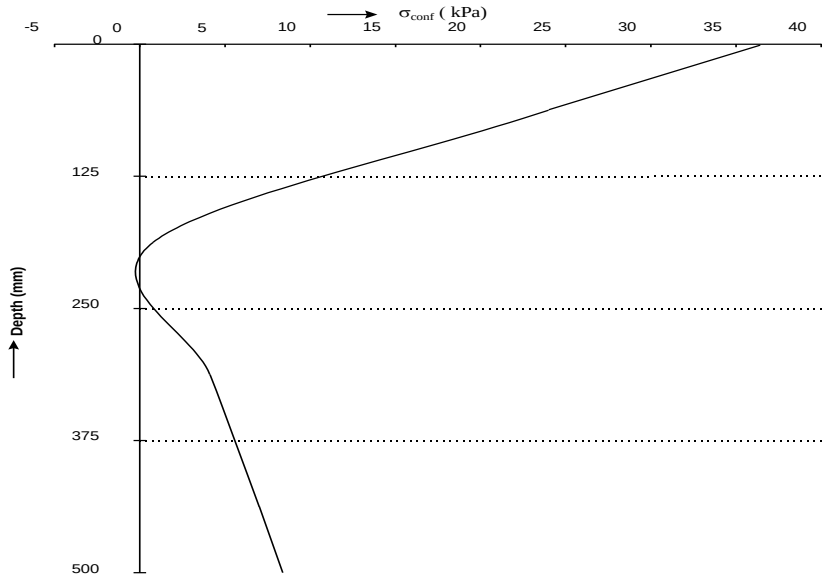

Figure 4.3 σ_{conf} as a function of the depth

4.3 Bisar iterations considering failure

As the previous attempts can't provide realistic stiffnesses the stiffness will be computed in an iterative manner using the linear-elastic multi-layer program Bisar and the Mohr-Coulomb failure criteria.
Before starting the calculations a few remarks regarding the load are given:

In figure 4.4 a sketch is drawn illustrating the relationship between the thickness of the base, the wheel load and the stiffness of the subsoil.
Suppose the wheel load has a value of A. When a subsoil stiffness of 50 MPa is considered the corresponding thickness must have a value of at least B. A base thinner than value B can't be applied because the structure won't be able to bear it. A structure with a subsoil stiffness lower than 50 MPa won't be able to carry the load A. Load A can be applied on a subsoil with a stiffness of 25 MPa or 50 MPa only if the base thickness has as at least a value of C or D respectively.

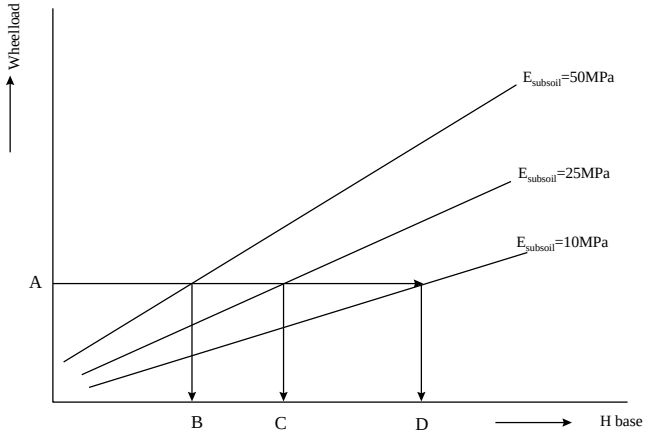

Figure 4.4 Applicable wheel load versus base thickness and subsoil stiffness

The idea behind this figure is that the stiffer the subsoil, the higher the wheel load can be, with a constant base thickness. Thinner bases would mean lower allowable wheel loads.
For most of the cases in this study a wheel load of 50 kN can't be applied to the structure (paragraph 4.7 and annex 2.6 will show that the load of 50 kN is indeed too heavy for the structure). Because of this from now on an average wheel load of 25 kN on a contact area of 106 mm will be used (for all the cases) in this survey.
The question which arises is "Can the structure bear the load?". The answer to this question can be found in paragraph 4.5.1 and 4.6. It will appear that for the thinner bases and the weakest subsoil the load is too big

Below an outline of the iteration procedure is given:

Step 1
Estimate a starting modulus for the sublayers. This is done using the Australian method. A modulus ratio of 2 will be used, this implies that the stiffness of the lower sublayer is $2*E_{subsoil}$. This is also done for the next sublayers (also 2 times the lower laying layer).

Step 2
Run the calculations with Bisar. Calculate the principal stresses in the middle of each sublayer.

Step 3
Check if shear has occurred using (4.2):

$$\sigma_{1,f} = \frac{(1+\sin\phi)\cdot\sigma_{conf} + 2c\cdot\cos\phi}{1-\sin\phi}$$

where

$\sigma_{1,f}$	: σ_1 at failure according to Mohr-Coulomb	(kPa)
c	: cohesion	(kPa)
ϕ	: angle of internal friction	(^{0})
σ_{conf}	: confining pressure	(kPa)

If it appears that a layer has failed due to shear than the stiffness should be revised by trial an error (for most cases increasing the stiffness could be a solution).

Step 4
Continue with step 3 until their is no failure.

Step 5
Compute the resilient modulus of the base using:

$$M_r = 34\cdot\theta^{0.38} \qquad (4.7)$$

where

M_r	: the resilient modulus	(MPa)
θ	: sum of the principal stresses	(kPa)

Step 6
Go on with the iterations until E (input) $\approx M_r$ (output).

Since there is no formal iteration procedure the iterations done are on the basis of engineering judgement and done with trial and error.

Regarding the procedure described above, 2 extra limitations (see figure 4.5) are assumed:

1. The shear stress should be maximum 80% (because of load repetitions and safety) of the shear strength (the shear strength is dependent on the cohesion and the angle of internal friction). In formula form $\tau_{occurred}/\tau_{max} < 0.8$.

The figure can be divided in 4 sections:

- In the case that $\tau_{occured}/\tau_{max} < 0.5$ the shear stresses are very low, and $M_r = M_{r,max}$ is then calculated by means of equation 4.7.
- If it appears that $0.5 < \tau_{occured}/\tau_{max} < 0.8$ the occurring shear stresses are higher. The lower $\tau_{occurred}$ the bigger θ and therefore the bigger M_r will be.
- The third section is $0.8 < \tau_{occurred}/\tau_{max} < 1$. The safety factor of 0.8 has been exceeded. The occurred shear stress will be bigger compared with the first two sections, thus θ will be low and therefore the resilient modulus M_r will be smaller.
- The last part is $\tau_{occurred}/\tau_{max} = 1$ This means that the shear stress has the same value as the shear strength.

2. The modulus should always be bigger than the subsoil modulus. This limitation refers to the fourth section of the graph, $\tau_{occurred}/\tau_{max} = 1$.

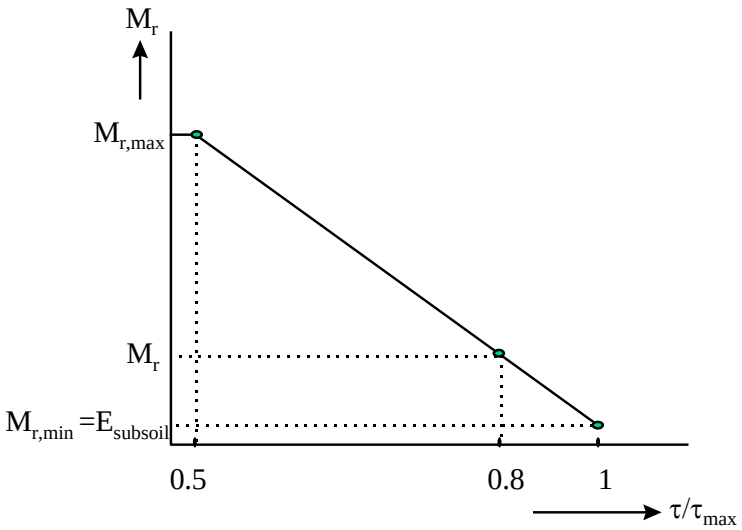

Figure 4.5 Limitations on M_r

4.4 Iterations for the 500 mm base

The base is divided in 4 layers, each with a thickness of 125 mm. In the next paragraph a summary will be given of the executed iterations.
In table 4.6 the input and the computed stresses with Bisar for the first iteration step are given. The calculations are done for all the cases in the middle of a sublayer in the centerline of the load. The output data in the tables is rounded.

4.4.1 The 10 MPa subsoil

Iteration step 1						
Layer	E (MPa)	σ_3 (kPa)	σ_1 (kPa)	σ_{selfw} (kPa)	$\sigma_{failure}$ (kPa)	M_r (MPa)
Sublayer 1	160	204	569	1.1	2507	-
Sublayer 2	80	-40	162	3.4	75	failure
Sublayer 3	40	-29	54	5.6	209	-
Sublayer 4	20	-12	25	7.9	401	-
subsoil	10	-	-	-	-	-

Table 4.6 Data for iteration step 1 (rounded)

The table is divided in 7 columns. In the first column the number of the sublayer is shown. In the second column the input value for the stiffness E, in the 3rd, 4th and the 5th column the horizontal, vertical and the stresses due to self weight are shown. The 6th column shows the maximum value for the vertical stress. This stress is computed with (4.2):

$$\sigma_{1,failure} = \frac{(1+\sin\phi)\cdot\sigma_{conf} + 2c\cdot\cos\phi}{1-\sin\phi}$$

Finally in the 7th column M_r is computed with equation 4.1.
The output in table 4.6 shows that layer 2 has failed (bold row) => $\sigma_{1,failure} > \sigma_1$. So the resilient modulus can't be computed and a next iteration is needed with different values for the E_{input}. The new input value for the stiffness must be bigger than the old one because the shear stress of the second sublayer is too high. How big this value should be is done by trial and error.
The next step can be seen in table 4.7.

Iteration step 2						
Layer	E (MPa)	σ_3 (kPa)	σ_1 (kPa)	σ_{selfw} (kPa)	$\sigma_{failure}$ (kPa)	M_r (MPa)
Sublayer 1	300	200	544	1.1	2466	459
Sublayer 2	98	-32	147	3.4	155	189
Sublayer 3	60	-30	50	5.6	198	67
Sublayer 4	35	-21	21	7.9	311	43
subsoil	10	-	-	-	-	-

Table 4.7 Iteration 2

Table 4.7 shows that none of the layers has failed. So the resilient modulus is computed. The new moduli are used as new input values for the next iteration step (iteration step 3, table 4.8).

Iteration step 3						
Layer	E (MPa)	σ_3 (kPa)	σ_1 (kPa)	σ_{selfw} (kPa)	$\sigma_{failure}$ (kPa)	M_r (MPa)
Sublayer 1	459	226	553	1.1	2728	-
Sublayer 2	189	-65	138	3.4	-176	failure
Sublayer 3	67	-28	41	5.6	218	-
Sublayer 4	*43*	*-23*	*17*	*7.9*	*291*	-
subsoil	10	-	-	-	-	-

Table 4.8 Iteration 3

Table 4.8 shows that layer 2 again fails. For layer 4 (italic values in table 4.8) calculation of M_r is not possible. This is because the sum of the principle stresses has a negative value of -5.3. This also has to be taken into account for the next iteration (table 4.9).

Iteration step 4						
Layer	E (MPa)	σ_3 (kPa)	σ_1 (kPa)	σ_{selfw} (kPa)	$\sigma_{failure}$ (kPa)	M_r (MPa)
Sublayer 1	450	192	519	1.1	2386	452
Sublayer 2	99	-34	125	3.4	135	166
Sublayer 3	58	-28	44	5.6	222	66
Sublayer 4	36	-21	19	7.9	303	34
subsoil	10	-	-	-	-	-

Table 4.9 Final iteration, $E_{subsoil}$ = 10 MPa

The output of table 4.9 shows that the input stiffness (column 2) is of the same magnitude compared with the output stiffness (column 7). In layer 2 the demand for the shear stress isn't reached and that $M_r = 1.7 \cdot E_{input}$. In this case $\tau_{occured}/\tau_{max} > 0.8$ but lower than 1 (also see figure 4.5).

In figure 4.6 the circles of Mohr are drawn for the stresses (including self weight) for the last iteration.

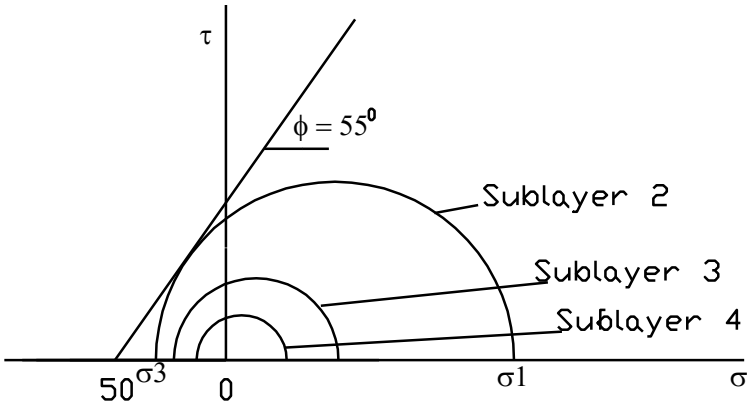

Figure 4.6 Circles of Mohr for the last iteration

4.4.2 The 25 MPa subsoil

Table 4.10 shows the output for the final stresses and stiffnesses for the 500 mm base on a 25 MPa subsoil. In figure 4.7 the circles of Mohr are presented for the last iteration step. In annex 2.3 an extensive output for this case is shown.

Final iteration						
Layer	E (MPa)	σ_3 (kPa)	σ_1 (kPa)	σ_{selfw} (kPa)	$\sigma_{failure}$ (kPa)	M_r (MPa)
Sublayer 1	450	195	555	1.1	ok	459
Sublayer 2	175	-31	157	3.4	166	198
Sublayer 3	100	-22	57	5.6	279	122
Sublayer 4	70	-19	26	7.9	331	86
subsoil	25	-	-	-	-	-

Table 4.10 Final iteration, $E_{subsoil}$ = 25 MPa

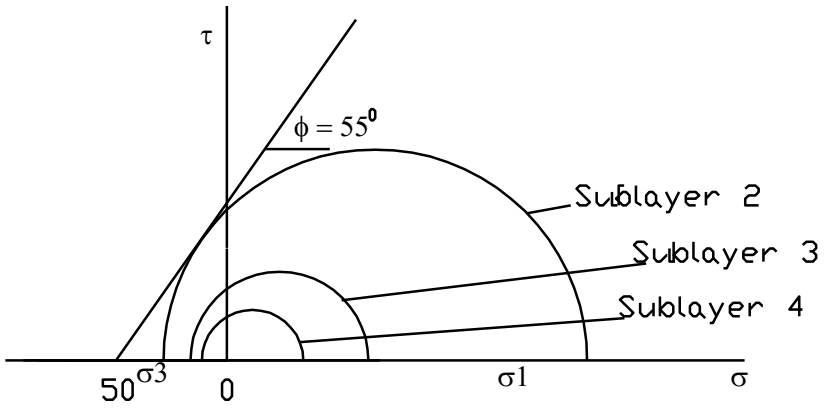

Figure 4.7 Circles of Mohr for the 25 MPa subsoil case

4.4.3 The 50 MPa subsoil

The output for the stresses and the computed moduli for the 50 MPa subsoil case are shown in table 4.11 and in figure 4.8 the circles of Mohr are drawn. The difference between input stiffness and output stiffness fluctuates between 2 and 6%. Because of the better subsoil properties it's easier to get low differences between input and output. A more detailed output is provided in annex 2.3.

Final iteration step						
Layer	E (MPa)	σ_3 (kPa)	σ_1 (kPa)	σ_{selfw} (kPa)	$\sigma_{failure}$ (kPa)	M_r (MPa)
Sublayer 1	450	186	573	1.1	ok	459
Sublayer 2	225	-19	181	3.4	135	230
Sublayer 3	155	-19	68	5.6	222	146
Sublayer 4	110	-16	32	7.9	303	113
subsoil	50	-	-	-	-	-

Table 4.11 Final iteration, $E_{subsoil}$=50 MPa

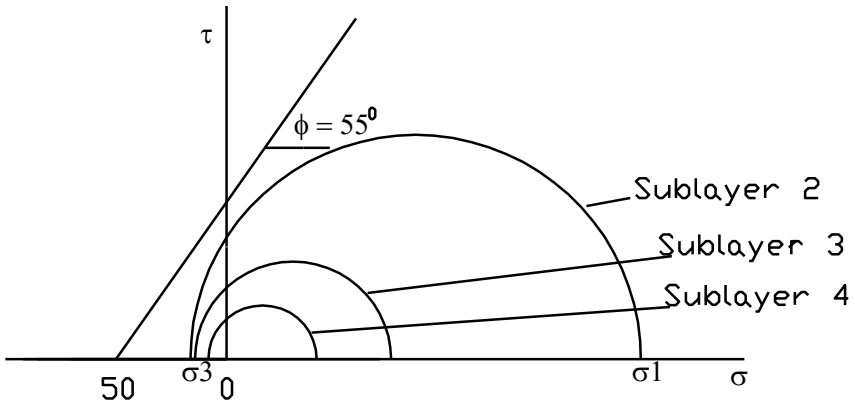

Figure 4.8 Circles of Mohr for the 50 MPa subsoil case

4.5 Iterations for the 350 mm base

The 350 mm base is divided in 4 sublayers of 100, 100, 75 and 75 mm each. In paragraph 4.5.1 the iteration steps are shown for the 10 MPa subsoil case. From that paragraph it will become clear that it is very hard to reach a situation with satisfying stiffnesses. The output for the other two cases (25 MPa and 50 MPa subsoil stiffness) are discussed in paragraph 4.5.2 and in annex 2.4.

4.5.1 The 10 MPa subsoil

In column 2 of table 4.12 the input values for the first iteration are shown. The output shows that layer 2 and layer 3 have failed ($\sigma_{failure}$ has been exceeded, the bolded values in the table).

Iteration step 1						
Layer	E (MPa)	σ_3 (kPa)	σ_1 (kPa)	σ_{selfw} (kPa)	$\sigma_{failure}$ (kPa)	M_r (MPa)
Sublayer 1	120	268	592	0.9	ok	-
Sublayer 2	50	-38	220	2.7	90	failure
Sublayer 3	30	-34	96	4.3	144	failure
Sublayer 4	23	-32	54	5.6	178	-
subsoil	10	-	-	-	-	-

Table 4.12 Iteration 1

A next iteration step with different input stiffnesses is needed until there is no failure anymore.

Iteration step 2						
Layer	E (MPa)	σ_3 (kPa)	σ_1 (kPa)	σ_{selfw} (kPa)	$\sigma_{failure}$ (kPa)	M_r (MPa)
Sublayer 1	600	208	480	0.9	ok	450
Sublayer 2	46	-25	119	2.7	219	177
Sublayer 3	34	-31	59	4.3	175	81
Sublayer 4	23	-23	36	5.6	268	71
subsoil	10	-	-	-	-	-

Table 4.13 Iteration 2

The second iteration (table 4.13) shows that none of the layers has failed. So the resilient modulus is computed.
The output of step 2 is needed as input for iteration step 3 in table 4.14.

Iteration step 3						
Layer	E (MPa)	σ_3 (kPa)	σ_1 (kPa)	σ_{selfw} (kPa)	$\sigma_{failure}$ (kPa)	M_r (MPa)
Sublayer 1	450	320	582	0.9	ok	-
Sublayer 2	177	-75	191	2.7	< 0	failure
Sublayer 3	81	-54	69	4.3	< 0	failure
Sublayer 4	71	-70	30	5.6	< 0	failure
subsoil	10	-	-	-	-	-

Table 4.14 Iteration 3

It isn't possible to compute for the sublayers 2, 3 and 4 the M_r modulus because the confining tensile stress σ_3 is exceeding the tensile strength of 50 kPa (the intercept value of the Coulomb failure curve with the vertical axis). The input E has also unrealistic values: the stiffness of the 4th layer is 7 times bigger than the subsoil modulus.
In the next step the modulus of the lower layers will be decreased and the modulus of the top layer will be increased.

Iteration step 4						
Layer	E (MPa)	σ_3 (kPa)	σ_1 (kPa)	σ_{selfw} (kPa)	$\sigma_{failure}$ (kPa)	M_r (MPa)
Sublayer 1	1000	217	470	0.9	ok	-
Sublayer 2	71	-45	100	2.7	18	failure
Sublayer 3	37	-30	47	4.3	185	-
Sublayer 4	26	-23	29	5.6	258	-
subsoil	10	-	-	-	-	-

Table 4.15 Iteration 4

From table 4.15, iteration step 4 it can be concluded that when the modulus of the toplayer is increased, this will lead to lower vertical stresses. In the next step (table 4.16) the stiffness of layer 1 is made even bigger.

Iteration step 5						
Layer	E (MPa)	σ_3 (kPa)	σ_1 (kPa)	σ_{selfw} (kPa)	$\sigma_{failure}$ (kPa)	M_r (MPa)
Sublayer 1	1400	197	451	0.9	ok	440
Sublayer 2	69	-38	83	2.7	89	96
Sublayer 3	36	-25	41	4.3	235	57
Sublayer 4	26	-21	26	5.6	289	41
subsoil	10	-	-	-	-	-

Table 4.16 Iteration 5

From table 4.16 it can be concluded that if the modulus of the toplayer is increased the vertical stresses of the layers beneath decrease and there'll be no failure in the other sublayers at all.
In the next step (6, table 4.17) the output of step (5) is used as input values for step 6.

Iteration step 6						
Layer	E (MPa)	σ_3 (kPa)	σ_1 (kPa)	σ_{selfw} (kPa)	$\sigma_{failure}$ (kPa)	M_r (MPa)
Sublayer 1	440	279	545	0.9	ok	-
Sublayer 2	96	-54	168	2.7	< 0	failure
Sublayer 3	57	-50	68	4.3	θ negative	-
Sublayer 4	41	-47	34	5.6	θ negative	-
subsoil	10	-	-	-	-	-

Table 4.17 Iteration 6

Table 4.17 shows that layer 2 has failed and that it isn't possible to compute θ for the 3rd and 4th layer because it has a negative value (for the 3rd sublayer this is -19 and for the 4th sublayer is this -43). The horizontal stresses are too big. The vertical stresses also have very high values just as in step 3.
It can be concluded that for a road with a 350 mm base on a 10 MPa subsoil the iterations can't provide acceptable results for a 25 kN wheel load. In paragraph 4.1 (figure 4.4) this has already been discussed. The load is to heavy for the road to carry it. An option would be lowering the load or use better aggregate material with better properties.

4.5.2 The 25 MPa and 50 MPa subsoil

In table 4.18 the final iteration steps are shown for the 25 MPa and the 50 MPa subsoil case. Figure 4.9 shows the circles of Mohr corresponding to the last iteration step.

Final iteration step for the 25 MPa subsoil						
Layer	E (MPa)	σ_3 (kPa)	σ_1 (kPa)	σ_{selfw} (kPa)	$\sigma_{failure}$ (kPa)	M_r (MPa)
Sublayer 1	500	247	550	0.9	ok	477
Sublayer 2	110	-27	187	2.7	199	221
Sublayer 3	82	-37	85	4.2	114	113
Sublayer 4	58	-30	49	5.6	198	66
subsoil	25	-	-	-	-	-
Final iteration step for the 50 MPa subsoil						
Layer	E (MPa)	σ_3 (kPa)	σ_1 (kPa)	σ_{selfw} (kPa)	$\sigma_{failure}$ (kPa)	M_r (MPa)
Sublayer 1	490	255	591	0.9	ok	487
Sublayer 2	192	-24	227	2.7	230	248
Sublayer 3	139	-33	103	4.2	154	148
Sublayer 4	102	-28	59	5.6	218	106
subsoil	50	-	-	-	-	-

Table 4.18 Final iteration for the 25 and 50 MPa subsoil

In the 2nd sublayer the ratio $\tau_{occured}/\tau_{max} \approx 1$. In these cases the sublayer hasn't met the "0.8" criterion for shear.
The structure with a subsoil of 25 MPa is on the edge of failure. This is concluded because it is very hard to reach a situation where $M_r = E_{input}$ for the 2nd sublayer.
In annex 2.4 an extensive output is presented.

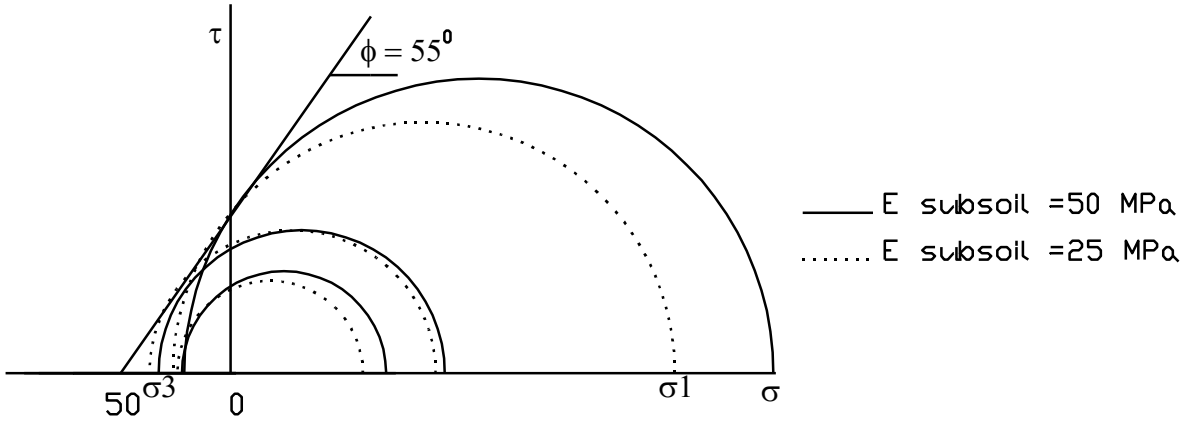

Figure 4.9 Circles of Mohr for the 350 mm base (layers 2, 3 and 4)

4.6 The 200 mm thick base

The 200 mm base structure is divided in 5 sublayers, a top layer of 100 mm and 4 layers of 25 mm each. For the results see table 4.19. For an extensive output see annex 2.5.

Final iteration step for the 10 MPa subsoil						
Layer	E (MPa)	σ_3 (kPa)	σ_1 (kPa)	σ_{selfw} (kPa)	$\sigma_{failure}$ (kPa)	M_r (MPa)
Sublayer 1	2000	134	412	0.9	ok	405
Sublayer 2	49	-32	59	2.0	152	45
Sublayer 3	37	-27	48	2.5	197	44
Sublayer 4	30	-24	41	2.9	233	29
Sublayer 5	25	-23	35	3.4	246	15
subsoil	10	-	-	-	-	-
Final iteration step for the 25 MPa subsoil						
Layer	E (MPa)	σ_3 (kPa)	σ_1 (kPa)	σ_{selfw} (kPa)	$\sigma_{failure}$ (kPa)	M_r (MPa)
Sublayer 1	2500	154	431	0.9	ok	418
Sublayer 2	100	-37	87	2.0	92	105
Sublayer 3	79	-33	70	2.5	137	89
Sublayer 4	66	-31	58	2.9	162	66
Sublayer 5	55	-28	50	3.4	196	58
subsoil	25	-	-	-	-	-
Final iteration step for the 50 MPa subsoil						
Layer	E (MPa)	σ_3 (kPa)	σ_1 (kPa)	σ_{selfw} (kPa)	$\sigma_{failure}$ (kPa)	M_r (MPa)
Sublayer 1	2800	167	450	0.9	ok	433
Sublayer 2	150	-30	116	2.0	162	163
Sublayer 3	130	-31	94	2.5	157	136
Sublayer 4	115	-32	77	2.9	152	109
Sublayer 5	99	-31	66	3.4	166	93
subsoil	50	-	-	-	-	-

Table 4.19 Final iteration for the 10, 25 and 50 MPa subsoil

It can be concluded that for the 200 mm base the 25 kN wheel load is to heavy. It is not possible to obtain satisfying results.
Table 4.20 shows for which cases it was possible to calculate the base stiffness.

Base thickness / Subsoil	500 mm	350 mm	200 mm
10 MPa	yes	no	no
25 MPa	yes	yes	no
50 MPa	yes	yes	no

Table 4.20 The cases for which the stiffness could/could not be determined

In the next chapter the calculated stiffnesses will be used as one of the input parameters for the FEM analyses with CAPA.

4.7 The 500 mm base, 50 kN wheel load

In this paragraph a summary is given of the iterations for the 50 kN wheel load.
In table 4.20 the output is presented for 4 iterations.
Each row of the table with data represents an iteration step. The 4th row represents the first iteration step with the 4 input stiffnesses (column 1 till 4), further to the right the computed stresses are shown for the different sublayers and in the last 4 columns the computes moduli are shown. These moduli are used as input for the next step.
It will be clear that for the other cases (lower subsoil stiffness and/or a thinner base) the structure will not be able to carry the load of 50 kN. The lower the subsoil stiffness the more difficult it will be to obtain a satisfactory end stiffness (see table 4.22 and annex 2.6).

Relevant Iterations; $E_{subsoil}$=50 MPa (stresses in kPa)															
Input Stiffness MPa				Stresses Layer 1		Stresses Layer 2		Stresses Layer 3		Stresses Layer 4		Output Mr MPa			
E_1	E_2	E_3	E_4	σ_3	σ_1	σ_3	σ_1	σ_3	σ_1	σ_3	σ_1	M_1	M_2	M_3	M_4
450	200	140	110	299	615	-18	278	-28	124	-25	63	505	278	183	121
505	278	183	121	316	626	-24	284	-40	119	-32	58	Failure			
505	278	165	121	317	625	-31	279	-34	118	-32	58	Failure			
475	240	165	121	308	622	-19	284	-34	122	-33	60	510	280	172	102

Table 4.21 Output 4 iteration steps for the 50 MPa subsoil case

In figure 4.10 the circles of Mohr are drawn for the last iteration. The figure shows that there is no failure.

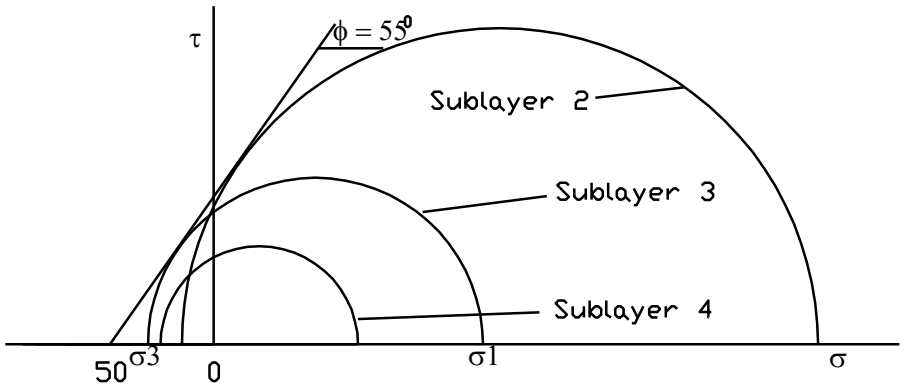

Figure 4.10 Circles of Mohr for the 50 MPa subsoil case

Relevant Iterations; $E_{subsoil}$=10 MPa (stresses in kPa)															
Input Stiffness MPa				Stresses Layer 1		Stresses Layer 2		Stresses Layer 3		Stresses Layer 4		Output Mr MPa			
E_1	E_2	E_3	E_4	σ_3	σ_1	σ_3	σ_1	σ_3	σ_1	σ_3	σ_1	M_1	M_2	M_3	M_4
75	40	30	20	300	627	-12	293	-35	128	-26	65	507	289	175	133
507	289	175	133	410	621	-70	249	-133	68	-25	25	Failure			
3500	95	49	34	211	143	-36	73	-25	36	-22	21	442	84	52	28
442	84	52	28	317	550	-51	195	-53	78	-31	38	Failure			

Table 4.22 Output 4 iteration steps for the 10 MPa subsoil case

Table 4.21 shows that in order to obtain a situation of no failure the stiffness of the first sublayer should be very high. A next iteration step immediately leads to failure.

Conclusion: the load is to big.

4.8 Concluding remarks

The usage of the method described in this chapter should be done with some care. Hereunder a few remarks regarding this method are made. Nevertheless it is believed that the method gives a good estimate for the base stiffness. On the other hand the output should be analyzed critically before it is used for further CAPA calculations.

- In general, unbound aggregate materials can't carry tension. In this case due to the high cohesion it's stated that tension can occur. A more likely Mohr failure shape is shown in figure 4.11. The tension area is very small (or even zero) compared with the extrapolated (dashed) one that has been used here.

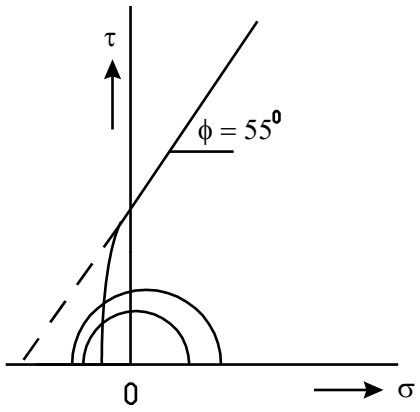

Figure 4.11 Mohr-coulomb failure line

- A remark regarding the M_r-θ method is illustrated in figure 4.12 and 4.13. The figures illustrates that the sum of the principal stresses for both cases are the same, but the stress conditions are different. In figure 4.12 the vertical stress (6) is smaller than in figure 4.13 (20). In fact the stress condition of figure 4.12 should give a higher stiffness but they both give the same, since θ has the same value of 2 for both cases.

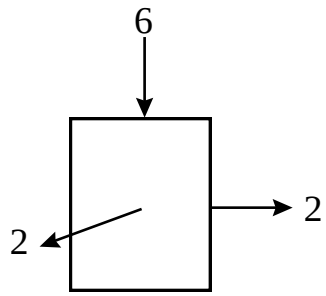

Figure 4.12 Case 1

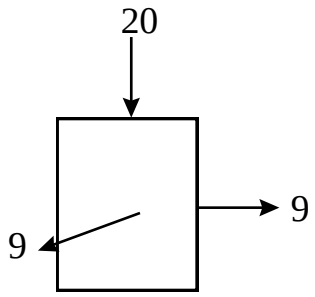

Figure 4.13 Case 2

- Another remark is that the stresses refer to the unfavorable case (the centerline of the load). The more you go to the sides the lower the stresses and the stiffnesses.

4.9 Conclusions

- Determination of the base stiffness with the program Kenlayer and using the M_r-θ material model gives no satisfactory output. The computed stiffnesses by the program Kenlayer are too high because the program Kenlayer sets all tension stresses to zero.

- In the M_r-σ_3-σ_1 model the essential second term is always one, because the failure term in the model is almost zero. The resilient modulus is dependent on the confining stress, σ_{conf}. The model is therefore comparable with the M_r-θ model and because the M_r-θ doesn't reckon failure, the model is because of this not suited.

- When the subsoil stiffness is increased, the applicable load can also be increased, and when the base thickness is reduced, the applicable load should also be reduced, else the structure can't bear the (high) load.

- The thinner the base, the lower the maximum load ought to be.

- Iterations done with Bisar, using an assumed relationship between the base stiffness and the occurring shear stress, give plausible M_r values.

- The assumed Mohr-Coulomb failure criterion for these cases is too optimistic (because in the base material tensile stresses are able to occur), but due to the high cohesion and the high angle of internal friction, to some extent tensile stresses are able to occur in the base material.

5. Finite Element Analyses with CAPA 2D

In this chapter the input parameters needed for CAPA 2D analyses are presented and discussed.

5.1 Parameters of influence

First the parameters of influence will be described. These are the bond stiffness and the type of reinforcement. The other parameters of influence, which have already been discussed in the previous chapters are: stiffness of the base, stiffness of the subsoil and thickness of the base.

5.1.1 Stiffness of the interlayer

For the analyses 2 types of reinforcement are considered:

1. A geogrid (EA = intermediate (5,000 N/mm))
2. A steelgrid (EA = high (50,000 N/mm))

Calculations are also done with no reinforcement. This is purely done as a reference. It will be clear that e.g. the stresses at the top of the subsoil are smaller when reinforcement is used. The effectiveness of the reinforcement is mainly dependent on the bond (see paragraph 5.1.2) between the reinforcement and the surrounding material.
The bond stiffness of grids is dependent on the size of the apertures, the stiffness of the junctions of the grid and the physical thickness.

5.1.2 The bond stiffness

The behaviour of the reinforcement depends on its type, the type of soil and the stress condition. These factors all have influence on the bond.
The bond is among other things dependent on the displacement of the reinforcement, the shear and normal stress in the interface and the material type (namely the size of the grids, the stiffness of the junctions, the shape of the surrounding material and the gradation of the aggregate material).

In CAPA 2D two types of material input data are needed for adequate simulation of the role of reinforcement:

1. Bond, shear stiffness (D_{tt})
2. Normal stiffness (D_{nn})

The constitutive relation between stress and displacements is defined as:

$$\begin{Bmatrix} \tau \\ \sigma \end{Bmatrix} = \begin{bmatrix} D_{tt} & 0 \\ 0 & D_{nn} \end{bmatrix} \cdot \begin{Bmatrix} s \\ w \end{Bmatrix} \qquad \textbf{(5.1)}$$

with

τ	: shear stress	(N/mm^2)
σ	: normal stress	(N/mm^2)
D_{tt}	: shear stiffness	($N/mm/mm^2$)
D_{nn}	: normal stiffness	($N/mm/mm^2$)
s	: slip (lateral)	(mm)
w	: deflection (normal)	(mm)

5.1.2.1 The normal stiffness D_{nn} and the shear stiffness D_{tt}

In this paragraph a relationship between D_{nn}, D_{tt}, the elastic modulus E and the shear (G) is derived.

In order to prevent the reinforcement from sinking into the subsoil, the normal stiffness of the interface element should have the same stiffness value as that of the base material. Due to the normal stiffness of the interface (D_{nn}) the construction reacts as if there were no discontinuity in the structure.
This means that there must be displacements compatibility between the interface element and the underlying base element.
Hereunder an analytic overview is given for the relation between D_{nn} and E.

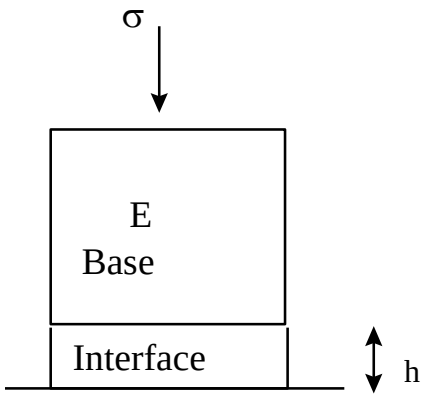

Figure 5.14 Interface element versus base

For the case of figure 5.1 compatibility of strains gives:

$$\varepsilon_{base} = \varepsilon_{int}$$

$$\sigma/E = w/h \qquad (5.1)$$

where w the vertical displacement of the interface.

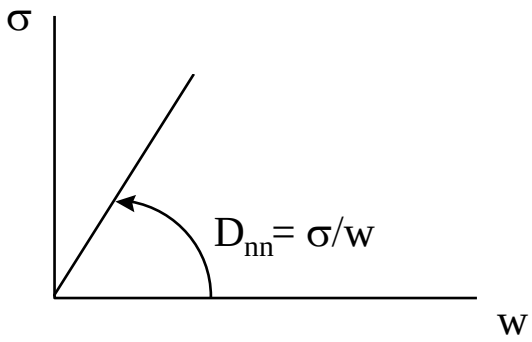

Figure 5.15 Physical relationship between σ, w and D_{nn}

By making use of the relationship of figure 5.2 formula (5.1) becomes:

$\sigma/E = 1/h \cdot \sigma/D_{nn}$

$\Rightarrow D_{nn}=E/h$ (5.2)

With h =1, D_{nn} = E.

The same procedure can be followed for the shear stiffness D_{tt}.

When a force is applied to the geotextile (figure 5.3) it is transferred to the surrounding material by means of bond stresses (figure 5.3 and 5.4). The slip of the reinforcement (s) is the horizontal displacement in relation to the surrounding materials.

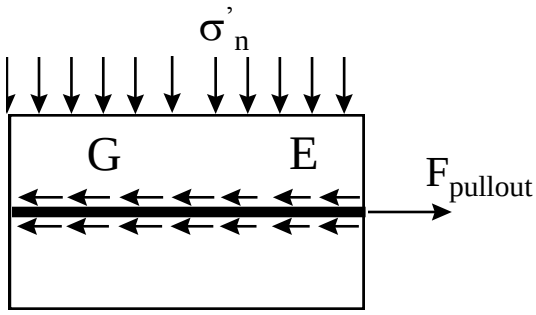

Figure 5.16 Pullout test

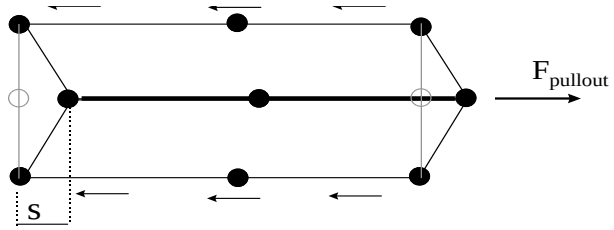

Figure 5.17 CAPA 2D bond model

The material adjacent to the reinforcement deforms in a shear mode as shown in figure 5.5.

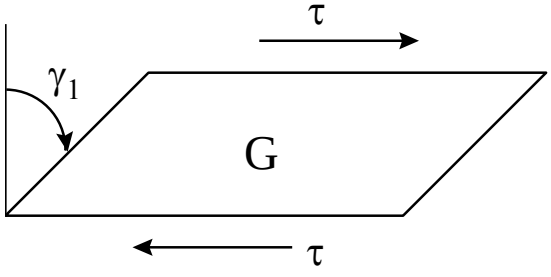

Figure 5.18 Shear aggregate

The shear strain in the aggregate further away from the reinforcement will be (see figure 5.5):

$$\gamma_1 = \frac{\tau}{G} \tag{5.3}$$

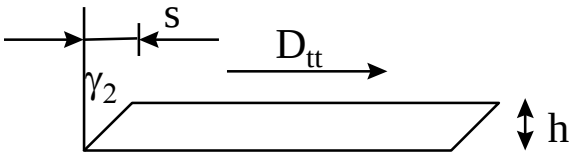

Figure 5.19 Shear geotextile

From figure 5.6, the strain in the aggregate adjacent to the reinforcement is:

$$\gamma_2 = \frac{s}{h} \tag{5.4}$$

For compatibility, $\gamma_1 = \gamma_2$, which leads to:

$$\frac{\tau}{G} = \frac{s}{h} \tag{5.5}$$

A physical relation between D_{tt}, τ and s is presented in figure 5.7.

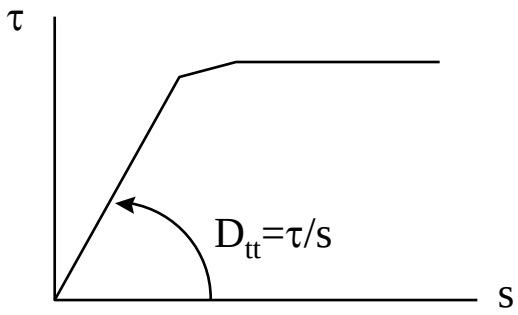

Figure 5.20 D_{tt} versus shear and slip

Substitution of $s = \tau/D_{tt}$ into equation 5.4 yields:

$$G\,\tau = D_{tt}\,h\,\tau$$

rewriting gives:

$$D_{tt} = \frac{G}{h} \tag{5.6}$$

With formula's 5.2 and 5.6 mathematical relationships between D_{nn}, D_{tt}, E, G and h are derived. Nevertheless, it must be pointed out that above computed values of D_{tt} correspond to the case of full strain compatibility between the reinforcement and the surrounding material. This is a highly unlikely situation and for this reason D_{tt} values must be computed on the basis of pullout tests as explained in the next section.

5.1.2.2 COI versus Dtt

Another way to describe bond (namely in the geomechanics) is by means of the Coefficient Of Interaction (COI). This COI is strongly related with friction. Friction is characterized as the relationship between the displacement of the interlayer and the shear stress in the interface. A test method used for the friction is a pull out test. The result is expressed by means of a coefficient of interaction (COI).

$$COI = \frac{\tau_{interface}}{\tau_{soil}} = \frac{F_{pullout} / 2 \cdot B \cdot L}{\sigma_n' \cdot \tan\phi} \qquad (5.7)$$

where :

$\tau_{interface}$	: shear strength in the interface	(kN/m^2)
τ_{soil}	: shear strength of the soil	(kN/m^2)
$F_{pullout}$	: pullout force	(kN)
B	: width of interlayer	(m)
L	: length of the interlayer	(m)
σ_n'	: normal stress	(kN/m^2)
ϕ	: internal friction angle	(^{o})

A value of 1 indicates full friction and a value of 0 will indicate full slip. For example: a membrane has low bonding (friction around 0.5). A material with big apertures (e.g. a steel grid) has higher bonding due to the better grip between the aggregate and the reinforcement (friction around 0.8) and the geogrid has an intermediate friction value of around 0.7.
The gaps of the grid should have a certain size related to the maximum size of the aggregate in order to optimize the bond. The same holds for the stiffness of the junctions. When this is high the bonding will be higher.

In table 5.1 some friction values are given as an indication.

Friction values COI for parameter study			
no reinforcement	0	0	0
geogrid (on top & below)	0.2	0.6	1
steelgrid (on top & below)	0.2	0.6	1

Table 5.1 COI values for friction

These friction values[3], given in table 5.1, are divided in a bond on the bottom of the base and one on top of the subsoil. It is assumed that the friction below the reinforcement as well as on top of the reinforcement has the same value. A COI of e.g. 1 means that both the top of the interface as well as the bottom of the interface have the same value of 1.
It should be realized that the friction values given should not be confused with the bond stiffness (D_{tt}, table 5.2) that is to be used in the FEM analysis.

[3] These values are obtained from "Survey in a pullout box regarding the friction behaviour of geotextiles in soil " by K. Maas, june 1994.

Considering the previous derivations for COI and D_{tt} a relation can be written out between them:

The relation for COI is:

$$COI = \frac{\tau_{interface}}{\tau_{soil}};$$

rewriting yields to:

$$\tau_{interface} = COI \cdot \tau_{soil}; \quad (5.8)$$

And the relation for D_{tt} is:

$$D_{tt} = \tau_{interface}/s \quad (5.9)$$

Substituting (5.8) into (5.9) gives:

$$D_{tt} = \frac{COI \cdot \tau_{soil}}{s};$$

$$D_{tt} = \frac{COI \cdot \sigma_n' \cdot \tan\phi}{s} \quad (5.10)$$

With (5.10) a relationship is derived between the bond stiffness, D_{tt}, and the Coefficient Of Interaction, COI.
A few remarks should be made considering this relation. The friction coefficient is derived at the pullout force and to calculate the D_{tt} only the slope of the pullout graph is needed. Furthermore the D_{tt} is dependent on the normal stress.
Figure 5.8 shows the relationship between COI and D_{tt}.

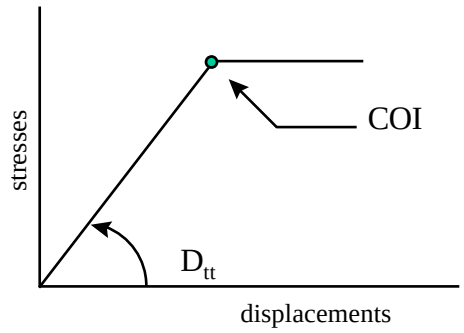

Figure 5.21 D_{tt} versus COI

The bond stiffnessess that were used for the parametric studies in this investigation are shown in table 5.2. It is assumed that for the cases with the grid and for the unreinforced cases the bond stiffness on the top as well as on the bottom of the interface have the same value. The unreinforced cases have a certain amount of bond, because there always will be an interaction (bond) between the layers. In order to compare the cases without reinforcement with the reinforced cases, the bond stiffnesses are the same for all the cases.

Different types of Bond (D_{tt}) for parameter study (N/mm/mm^2)			
no reinforcement	0.1	1	10
geogrid (on top & below)	0.1	1	10
steelgrid (on top & below)	0.1	1	10

Table 5.2 Bond values (D_{tt}) for parameter study

5.2 Parameter study

In table 5.3 and 5.4 the definite values for the parameter study are presented. The original parametric study has been adjusted.
Table 5.3 gives the values for the bond, the base thickness the type of subsoil and the type of reinforcement.
The value for $D_{nn}$is the same as the value of E_{yy} of the lowest base sublayer. Cross combinations are not done.

$E_{subsoil}$ (MPa)	Reinforcement (EA) (N/mm)	Base Thickness (mm)	D_{tt} (N/mm)/[mm]^2
10	geogrid (5,000)	200	0.1
25	steelgrid (50,000)	350	1
50	-	500	10

Table 5.3 Values for the parameter study

	350 mm		500 mm		
$E_{subsoil}$	25 MPa	50 MPa	10 MPa	25 MPa	50 MPa
Layer 1	500	490	450	450	450
Layer 2	110	192	99	175	225
Layer 3	82	139	58	100	155
Layer 4	58	102	36	70	110

Table 5.4 Stiffness of the base MPa

For the different combinations for the CAPA runs see annex 1.1.

6. Results

In this chapter the results of the parameter study are presented. In paragraph 6.1 first the input mesh (super elements) is given. In 6.2 and 6.3 it is made clear why complete isotropy ($E_{xx} = E_{yy}$) is not applicable for this structure. In paragraph 6.4 the influence of the neutral axis on the displacements is shown. In order to avoid a 4 layered base, whereby the base stiffness gradually decreases as the depth increases, in paragraph 6.5 an equivalent mesh is introduced. Finally in paragraph 6.6 and 6.7 the parameter study is presented.

6.1 Input mesh

The properties given in chapter 3 must be translated to a CAPA input mesh. In figure 6.1 this mesh is shown. This mesh correspondents to the 500 mm thick base on a subsoil which extends to infinity. Specially developed infinite elements have been utilized. To the side the subsoil also goes to infinity. The load is a line load with p = 0.707 MPa.
The mesh consists of 25 super elements and 37 super nodes. Furthermore only half the road is considered (instead of the whole 4500 mm only 2250 mm is considered, because of symmetry in the middle). In order to describe this the boundary on the right side is restrained. The nodes can only move in vertical direction (this is done by using rollers).

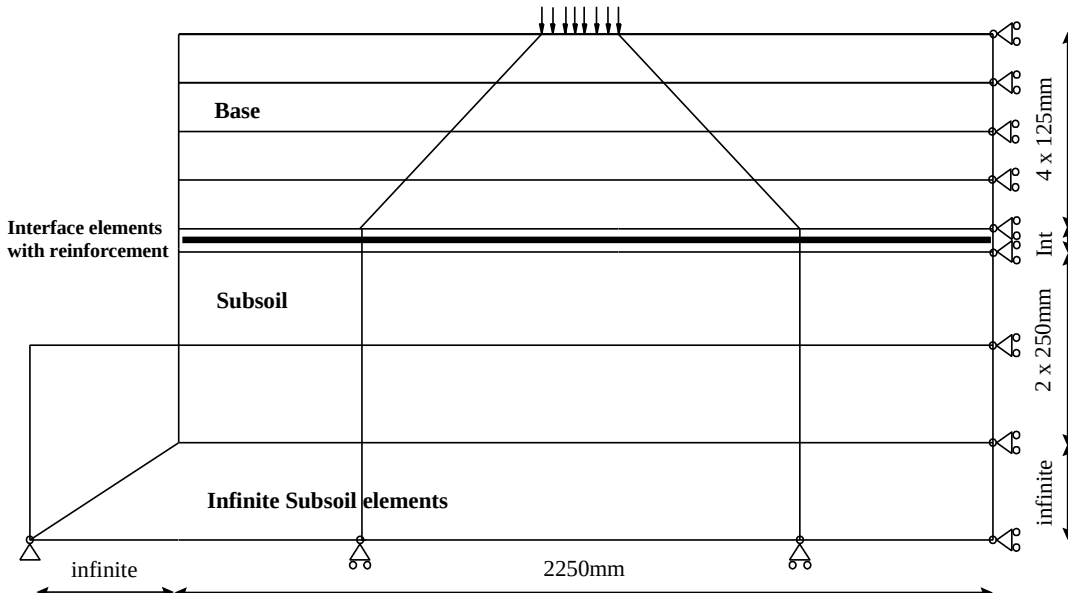

Figure 6.1 Input mesh (Schematic)

From the superelements mesh one can see that the elements under the load aren't rectangular. The reason for this is that the angle under which the load is spread (45^0) is also taken into account. In paragraph 6.3 will be elaborated on this matter.
Figure 6.2 shows the same mesh, but this time generated by CAPA. The generated mesh contains 495 nodes and 171 elements, this as comparison with the input mesh (these values are obtained from the CAPA output file).

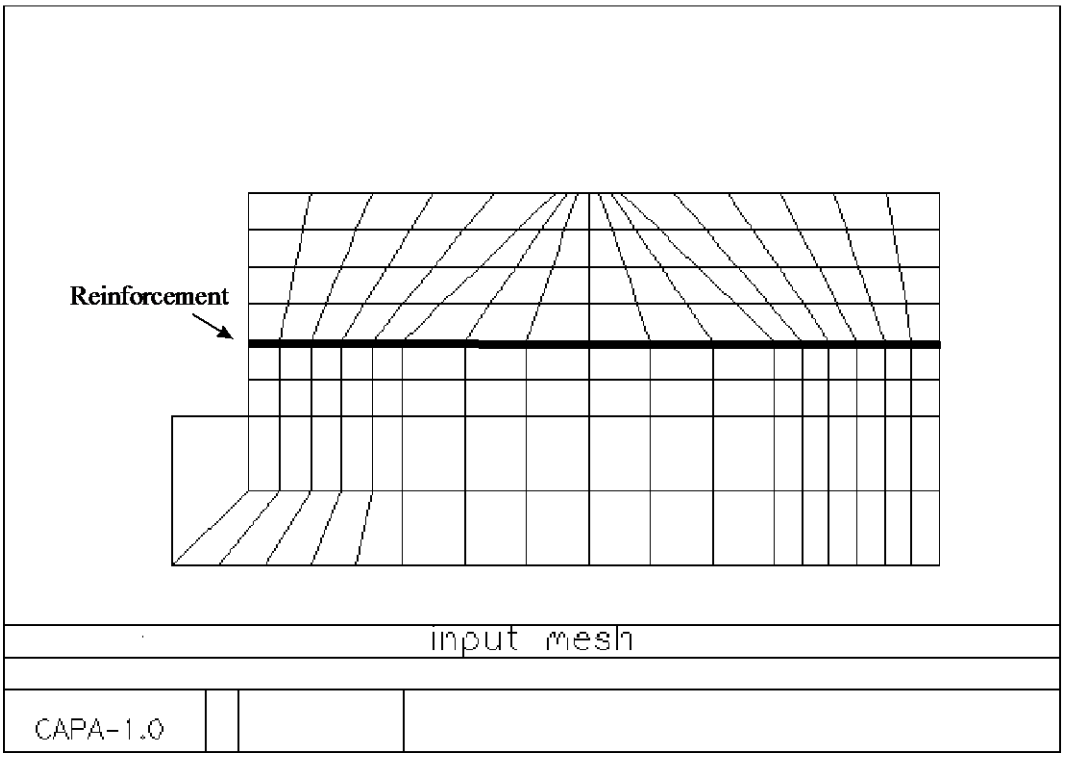

Figure 6.2 Generated mesh by CAPA

6.2 Isotropic analyses

In figure 6.3 the displacements for the interface/reinforcement are shown. The output shows that when $E_{xx} = E_{yy}$ there will be very little influence of the reinforcement on the displacements.
In the figure three cases are compared: a (geo)grid with EA=5,000 N/mm and a (steel)grid with EA=50,000 N/mm . The difference between no reinforcement at all and the stiff reinforcement is approximately 2.7%.

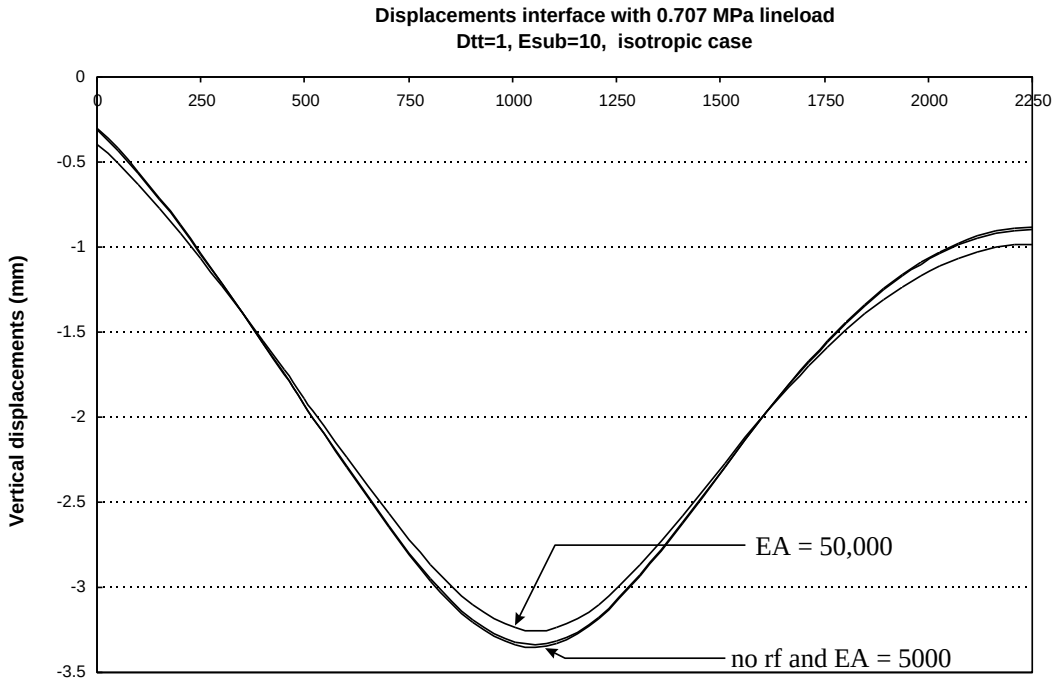

Figure 6.3 Vertical displacements at the interface

Figure 6.4 shows the development of the strains of the reinforcement. The strain goes from zero (left side, towards the edge of the road) to a maximum (center of the load) and decreases then to a negative value (compression) in road axis.

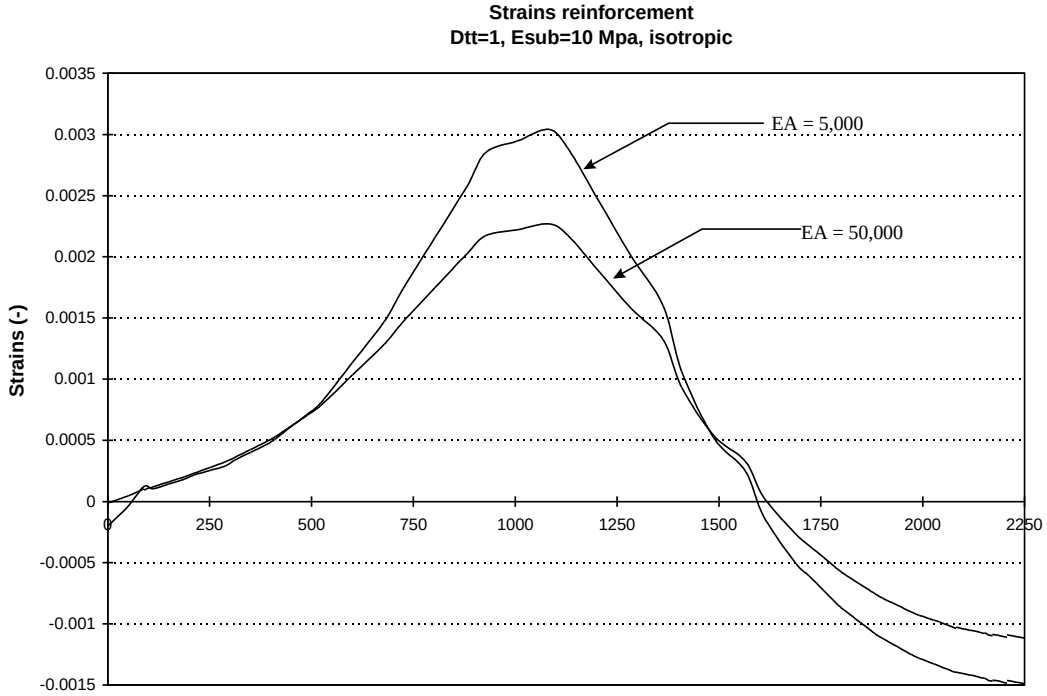

Figure 6.4 Strains in the reinforcement

It can be concluded that in the isotropic case the reinforcement isn't stretched significantly. Figure 6.4 shows little influence on the strain. The difference in strain between the two compared cases is low. The influence for the vertical displacements is therefore only 2.7% (see figure 6.3). When the case without the reinforcement is compared with the case with an EA 5,000 N/mm there is no influence at all for the displacements

The reason for the reinforcement not being stretched significantly is because of the ability of the structure to carry tension stresses.

The purpose of the reinforcement (take up tensile stresses) is diminished.

6.3 Partially anisotropic

The reinforcement will only work when the capability of the aggregate material to carry tension is diminished. As CAPA performs only linear analyses this has to be accounted for manually. The areas where tension will likely occur are made anisotropic ($E_{xx} \rightarrow 0$ and $G = E_{yy}/2$). These are the bending areas. In figure 6.5 these areas are hatched. They are in the top sublayer of the base and in the load spreading area of the load. The area directly under the load isn't made anisotropic due to high confining compression stresses. The subsoil is also made anisotropic, because it's unrealistic that tensile stresses can occur there.

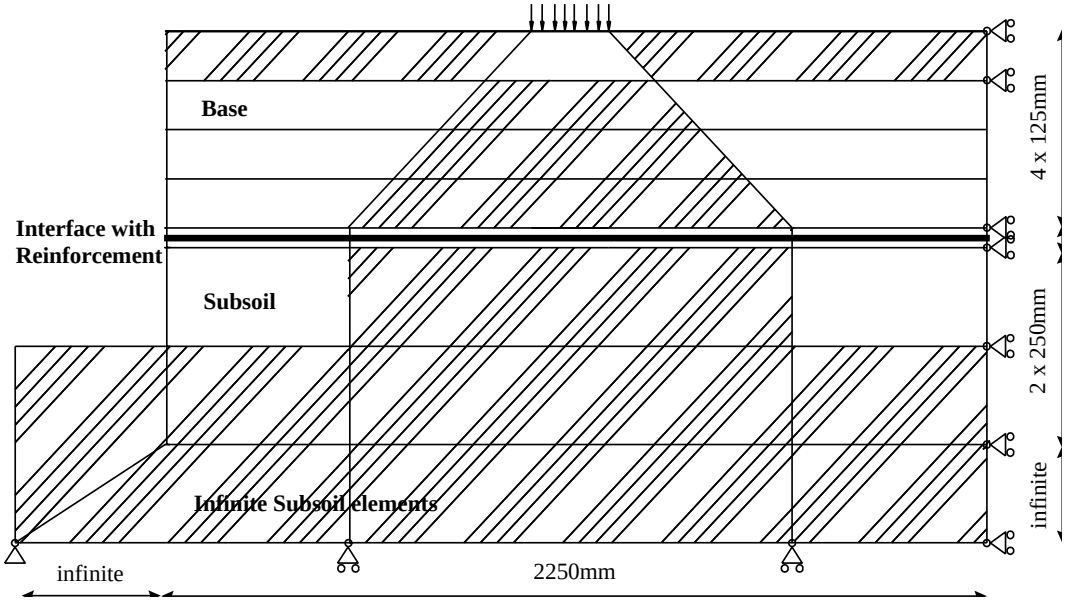

Figure 6.5 Mesh with the anisotropic (hatched) elements (Schematic)

Figure 6.6 shows the output for the deflections of the interface material for the 3 different cases (no reinforcement, medium EA and high EA).

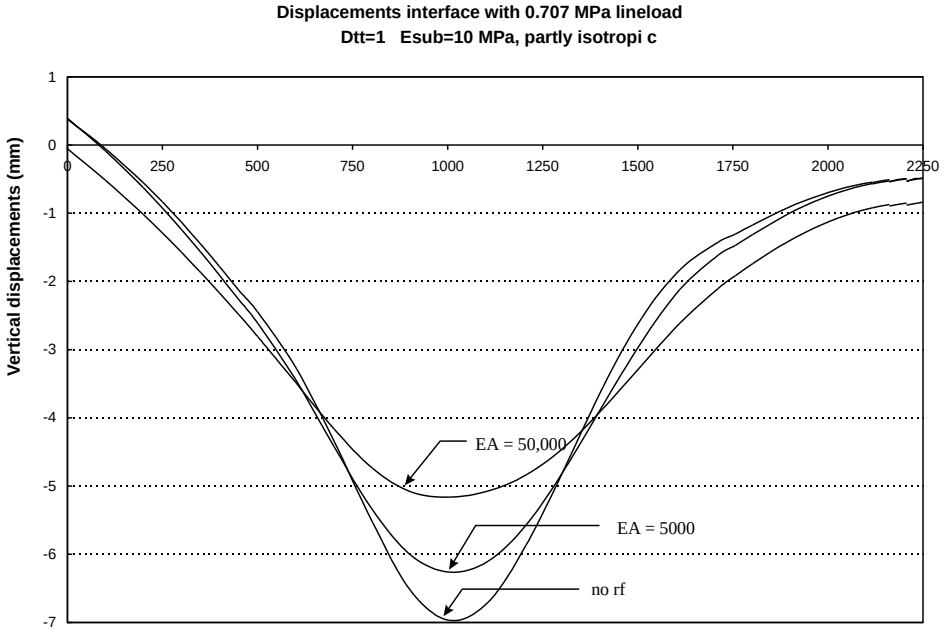

Figure 6.6 Vertical displacements at the interface, 10 MPa subsoil

Figure 6.7 shows for the same case the development of the strains in the reinforcement.
The difference in displacements between no reinforcement and the reinforced cases is a lot bigger compared with the isotropic case.

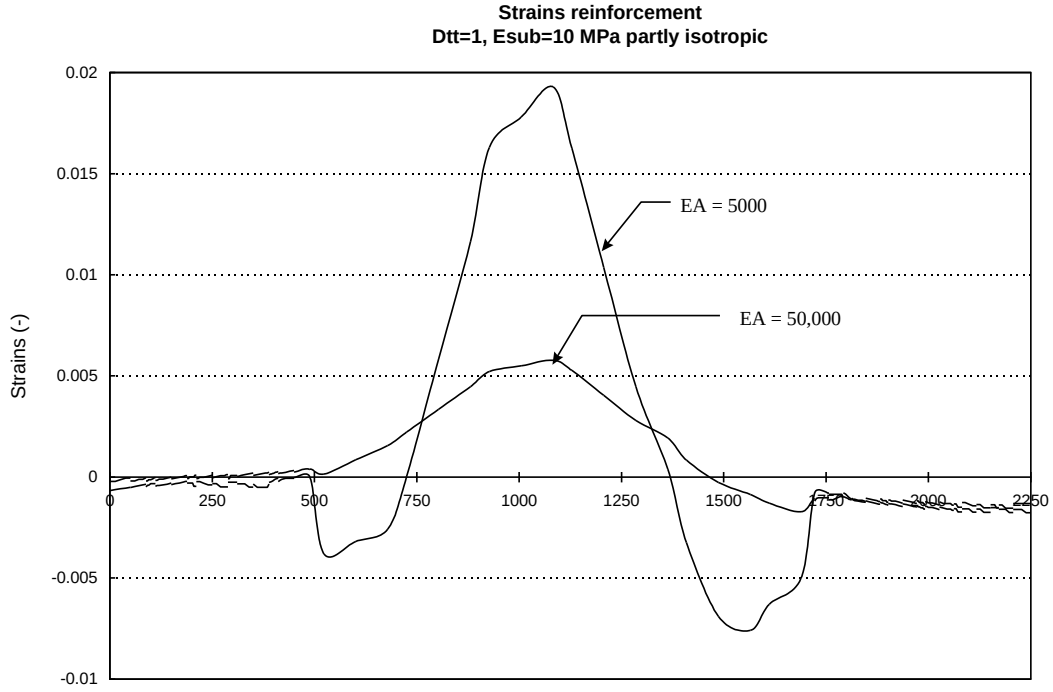

Figure 6.7 Strains in the reinforcement

The strain for the EA 50,000 N/mm case shows a discontinuity around x=500 mm and x=1500 mm. This is because in those areas the E_{xx} goes from zero to a value of 55 MPa. In contrast to this the isotropic case (figure 6.4) shows no discontinuity in the strain curve.

The conclusion is that when the ability of the structure to carry tension is taken away, the presence of a reinforcement immediately reduces the displacements (reduction of max. 27% when a grid with a high EA is used (a steel grid for example)).

Another factor of influence on the performance of the reinforcement is the position of the neutral axis. When the neutral axis lies high, the tension stress in the reinforcement will be bigger.
When the reinforcement is placed in the viscinity of the neutral axis it is useless.
This is illustrated in paragraph 6.5 with a simple beam where the reinforcement lies in the neutral axis and a case where the reinforcement lies below it.

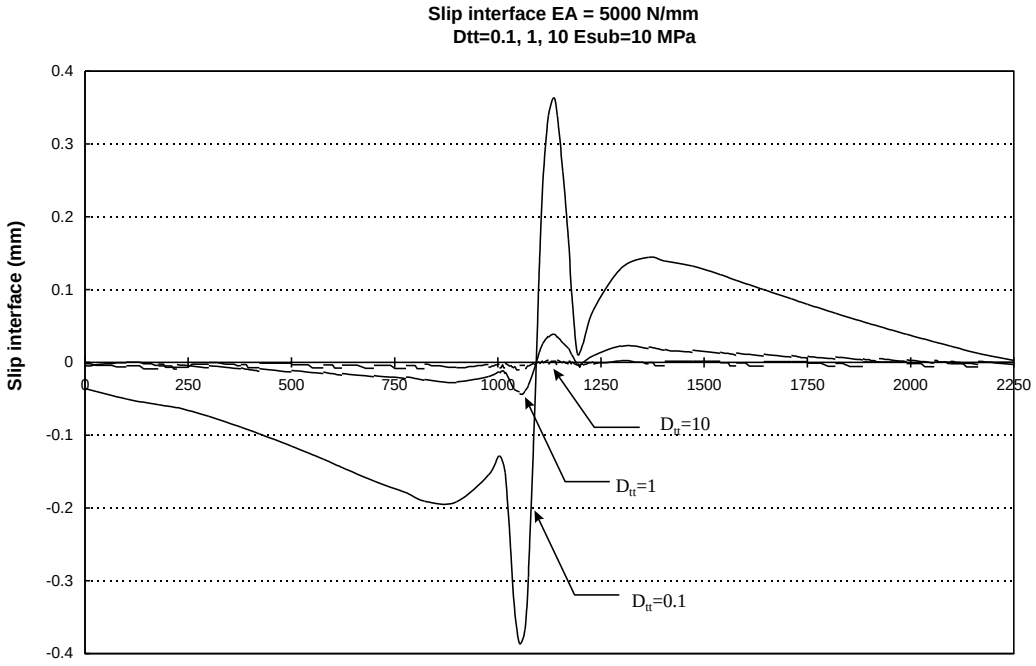

Figure 6.8 Influence of bond on slip of the interface (10 MPa subsoil)

Figure 6.8 shows the slip of the interface as a function on the bond stiffness D_{tt} for the case where the stiffness of the reinforcement, EA has a value of 5000 N/mm. Slip is defined as the horizontal displacement in relation to the surrounding materials (also see figure 5.4). The figure shows that an increase of D_{tt} leads to a decreases of the slip of the interface. The anchorage of the reinforcement is very small when D_{tt} is 0.1 N/mm/mm^2. In the middle of the line load the slip is 0 mm. In this point the orientation of interface elements changes.
Figure 6.9 shows the shear stresses in the interface for a stiffness of 5000 N/mm and 50,000 N/mm as a function of the stiffness of the reinforcement EA. The graph follows the same trend as that of the slip of figure 6.8. As the stiffness of the reinforcement increases, the shear stress will also increase. This is because of linearity.

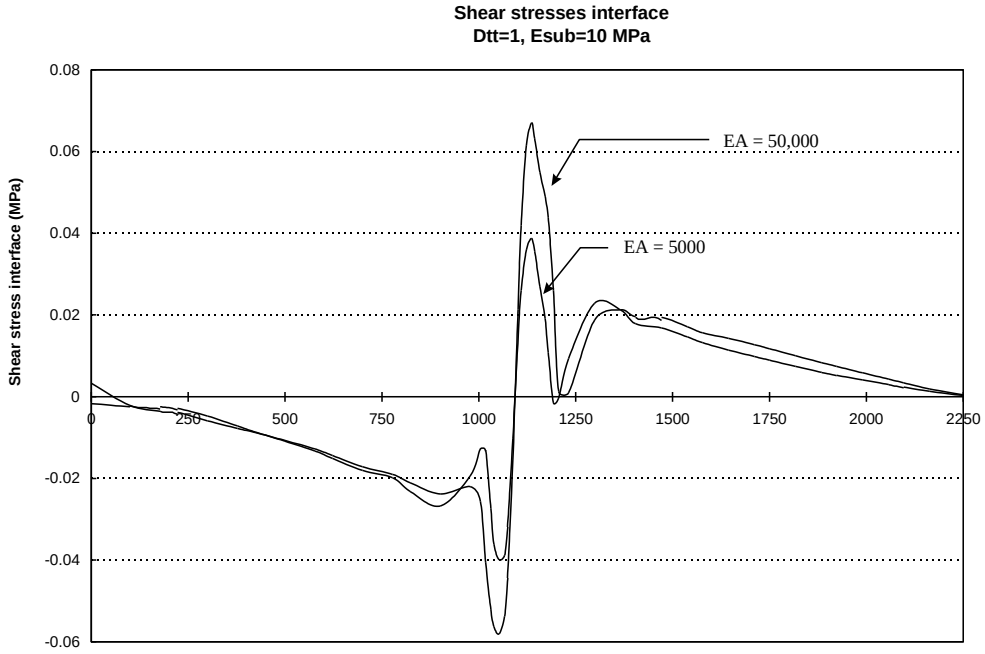

Figure 6.9 Influence of stiffness reinforcement on shear stress of the interface (10 MPa subsoil)

Instead of making the structure partly anisotropic the whole structure could have been made anisotropic. The disadvantage of this is that then the aggregate material can't transmit the forces to the interface. Anchorage is absent. The influence on the displacements will be smaller.
The output for this case is shown in annex 3.2.

This means that the isotropic areas (no bending, not hatched areas) in figure 6.5 are essential for the transmission of the forces into the reinforcement.

6.4 Equivalent mesh

In the previous paragraphs the base consisted of 4 sublayers. In order to reduce the amount of sublayers the base is divided in only 2 sublayers. In figure 6.10 the "new" super elements are shown. Now the mesh contains 19 super elements and 29 super nodes.

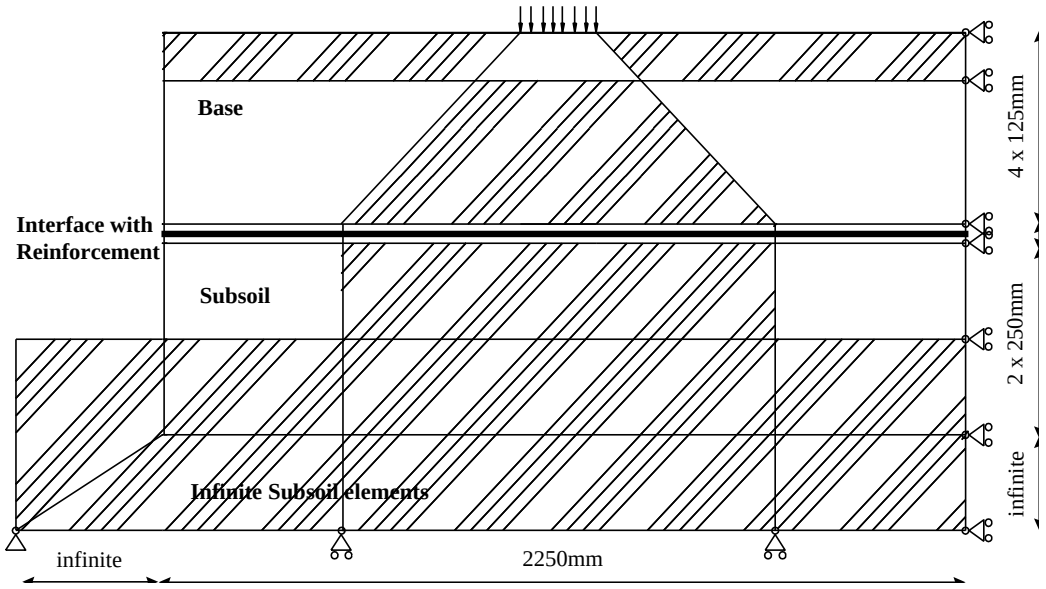

Figure 6.10 Equivalent mesh

Three sublayers are substituted with one layer (see figure 6.11). This means that the equivalent layer has a different stiffness. This new stiffness is only valid for the vertical displacements. Hereunder the derivation is given and in table 6.1 the new equivalent stiffnesses are given for the 500 mm and 350 mm base.

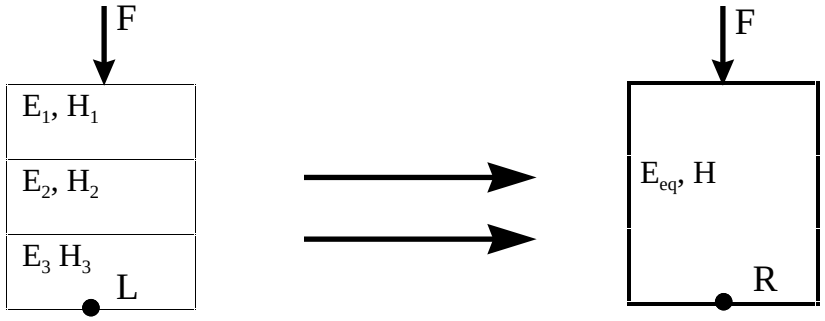

Figure 6.11 Transition from 3 layers to 1 layer

The condition for the displacements in point L and point R is:

$\delta_L=\delta_R$. => $\delta_1+\delta_2+\delta_3=\delta_R$

With $\sigma = E\cdot\varepsilon$ follows:

$A\sigma = E\,\varepsilon A$

Rewriting gives:

$$\Rightarrow \quad F = EA\frac{\delta}{H}$$

$$\Rightarrow \quad \delta = \frac{F \cdot H}{EA}$$

With A=1 m^2 this leads to

$$\frac{FH_{tot}}{E_{equ}} = \frac{FH_1}{E_1} + \frac{FH_2}{E_2} + \frac{FH_3}{E_3}$$

The final equation is:

$$\boxed{\frac{1}{E_{equ}} = \frac{H_1 / H_{tot}}{E_1} + \frac{H_2 / H_{tot}}{E_2} + \frac{H_3 / H_{tot}}{E_3}} \qquad (6.1)$$

In table 6.1 the "old" and the "new" equivalent stiffnesses are shown for the 500 mm thick base using equation 6.1.

H=500 mm (stiffness in MPa)				
	TOP-LAYER	**LOWER LAYER(S)**		
Subsoil =10 MPa				
"old" stiffness	450	99	58	36
equivalent stiffness	450	55		
Subsoil = 25 MPa				
"old" stiffness	450	175	100	70
equivalent stiffness	450	100		
Subsoil = 50 MPa				
"old" stiffness	450	225	155	110
equivalent stiffness	450	150		

Table 6.1 Equivalent stiffnesses for the 500 mm base

In paragraph 6.6.1 the 4-layered system (figure 6.6) and the 2-layered equivalent system (figure 6.16) are compared with each other on their correctness.

Table 6.2 shows the "old" and the "new" equivalent stiffnesses for the 350 mm base thickness.

H=350 mm (stiffness in MPa)				
	TOP-LAYER	**LOWER LAYER(S)**		
Subsoil =25 MPa				
"old" stiffness	500	110	82	58
equivalent stiffness	500	80		
Subsoil = 50 MPa				
"old" stiffness	490	192	139	102
equivalent stiffness	490	140		

Table 6.2Equivalent stiffnesses for the 350 mm base

6.5 Influence neutral axis

6.5.1 Reinforcement in neutral axis

Another very important observation is the position of the neutral axis. If the reinforcement lies exactly in this point (the point where the stresses are zero), the reinforcement will not be activated. (see figure 6.12 and 6.13).

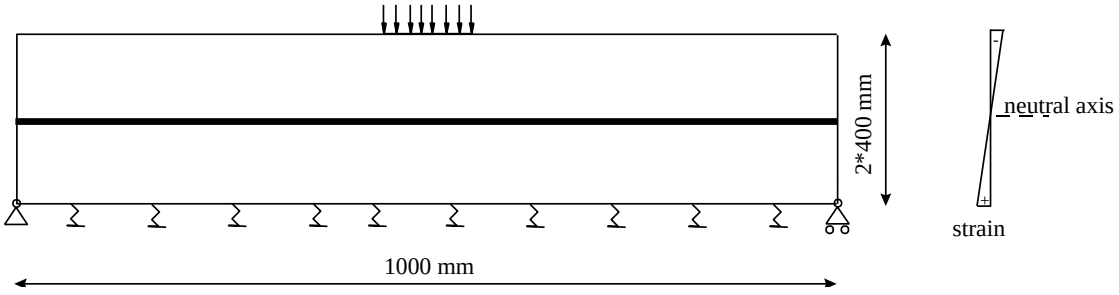

Figure 6.12 Reinforcement in neutral axis(not on scale)

To prove this a simple beam continuously supported, is analyzed with CAPA.
The beam has a length of 1000 mm and is 800 mm high. The reinforcement is placed exactly in the middle of the beam.

The input properties are:

E_{beam}	: 10	MPa
D_{tt}	: 0.5	$N/mm/mm^2$
EA	: 500,000, 10,000 and no reinforcement	N/mm

The output for the displacements for a 0.707 MPa line load is shown in figure 6.11.

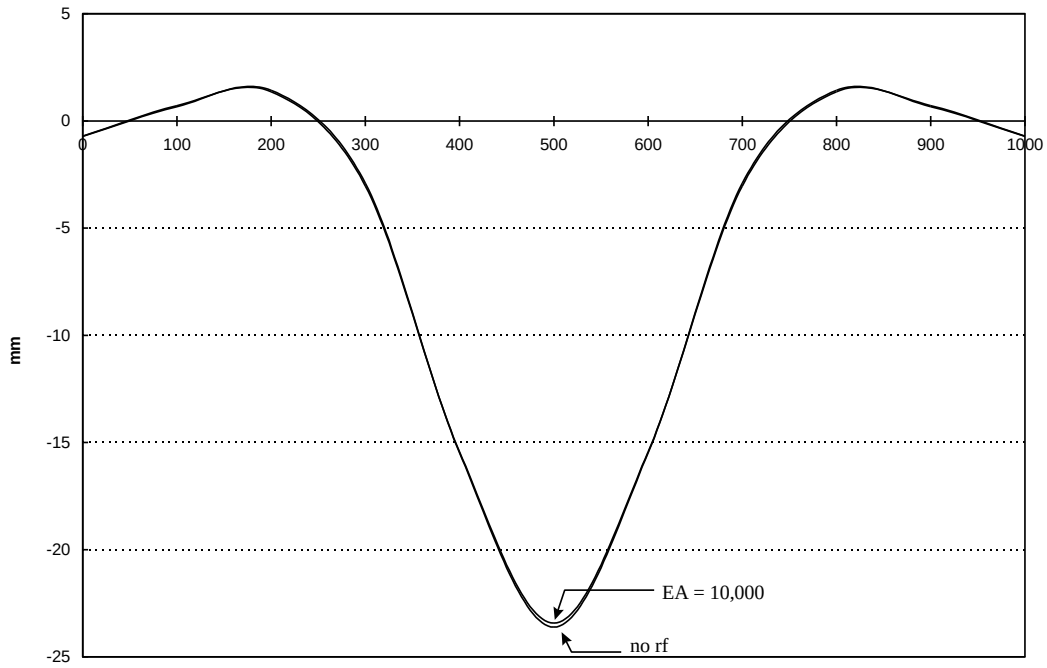

Figure 6.13 Vertical displacement (reinforcement lies in the neutral axis)

6.5.2 Reinforcement below neutral axis

In this case the reinforcement is transferred to a position below the neutral axis (figure 6.14). This means that applying the reinforcement will give lower vertical displacements.

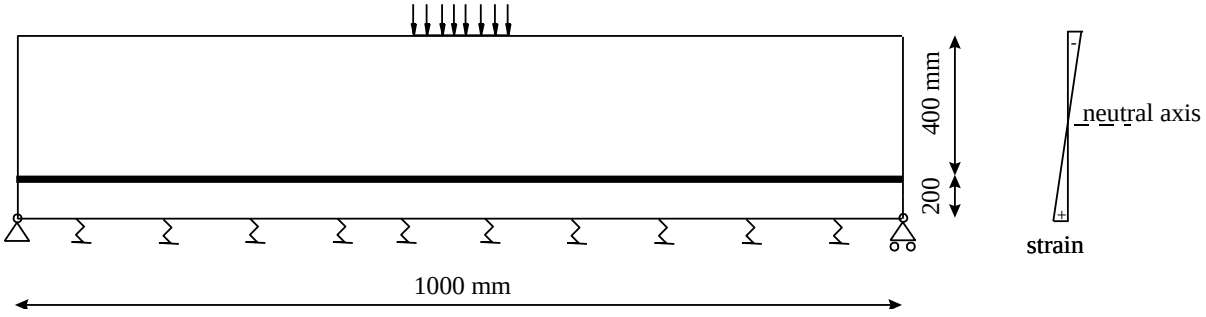

Figure 6.14 Reinforcement below neutral axis (not on scale)

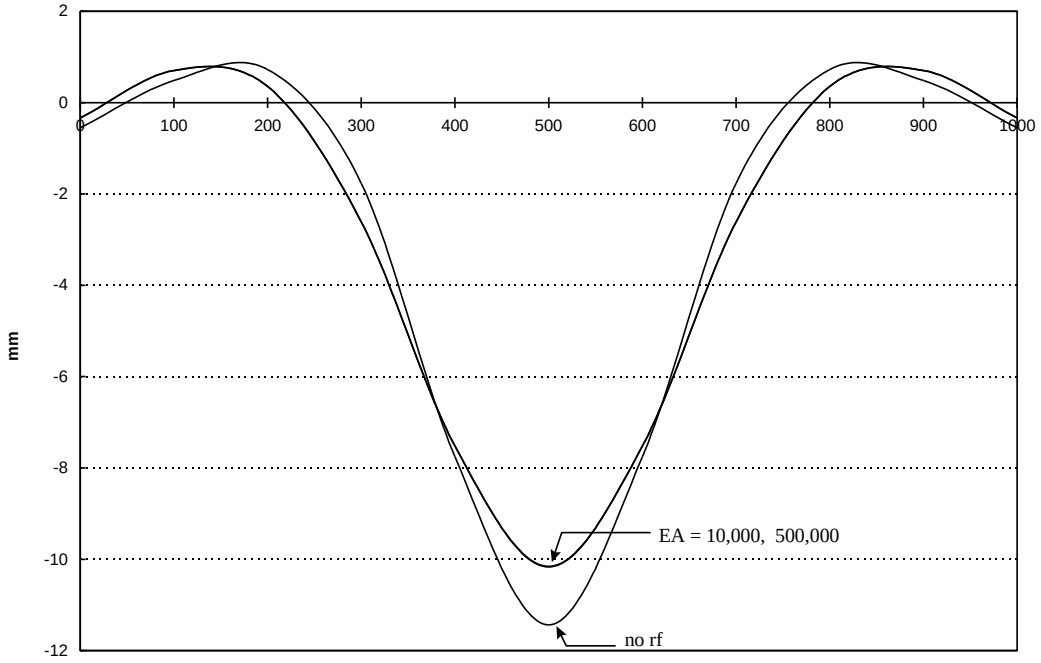

Figure 6.15 Vertical displacements (reinforcement below neutral axis)

From figure 6.15 it is concluded that if the reinforcement is placed in a position lower than the neutral axis the reinforcement begins to work.
When figure 6.15 and 6.13 are compared it can be seen that the displacements in figure 6.15 are smaller. The reason for this is that the reinforcement lies nearer to the bottom line.

Another conclusion which can be made is that above a certain stiffness (see figure 6.15) there will be no further decrease of the displacements anymore.
The weakest chain in that case is the stiffness of the interface. The displacements are settled by the stiffness of interface and not by the stiffness of the reinforcement.
For this case it means that an increase of stiffness of the reinforcement (to 500,000 N/mm) shows no further decrease of the displacements compared with the EA= 10,000 N/mm case.

6.6 Output parameter study for the 500 mm base

6.6.1 Output for the 10 MPa subsoil

From now on the CAPA runs are executed for the equivalent mesh with 2 sublayers for the base. Figure 6.14 shows the output for the displacements for the 10 MPa subsoil case.

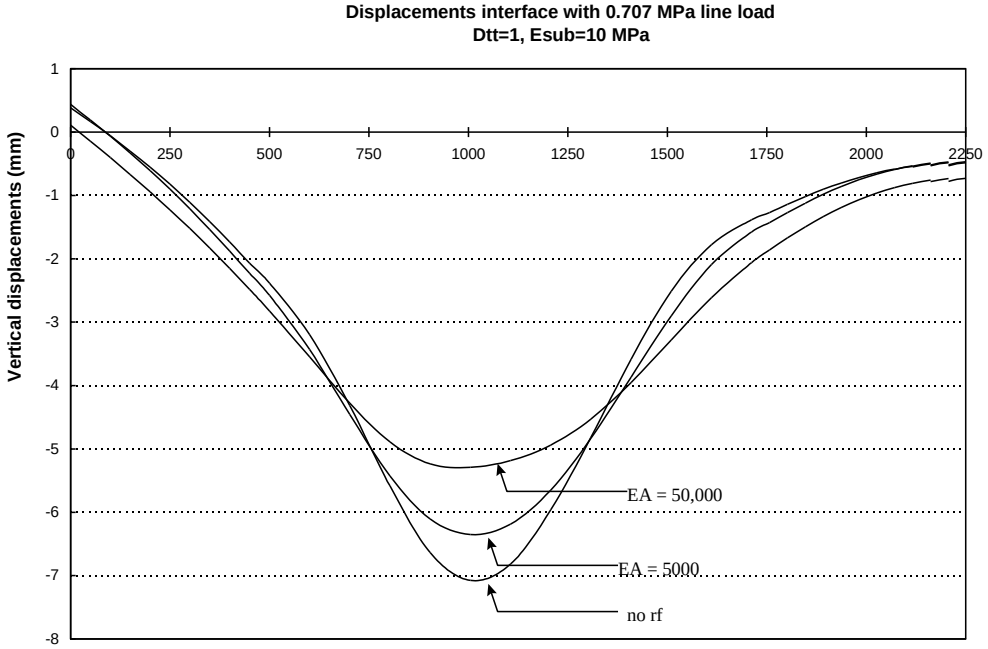

Figure 6.16 Vertical displacements at the interface, 10 MPa subsoil

The output shows that the displacements reduce with 10% and 25% for EA=5,000 N/mm and EA=50,000 N/mm respectively.
When the 4-layered (figure 6.6) case and the 2 layered case (figure 6.16) are compared with each other it can be seen that the displacement show differences of about 1%. Figure 6.17 shows the strains of the reinforcement.

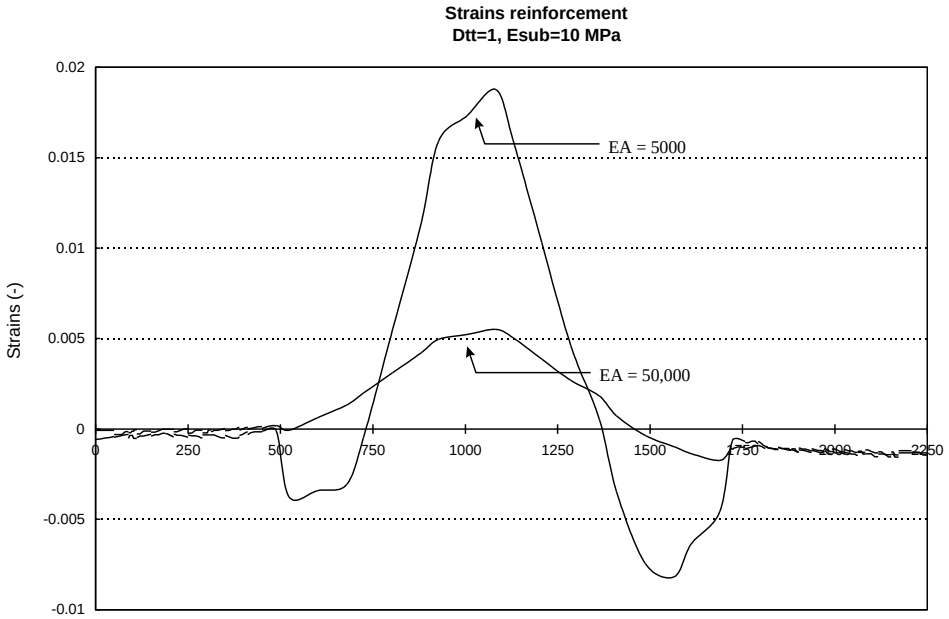

Figure 6.17 Strains in reinforcement as a function of EA for D_{tt}=1 N/mm/mm^2, subsoil 10 MPa

The maximum strain for the reinforcement with a EA of 5,000 N/mm is 1.88%. This value is acceptable since the maximum strain at yield for comparable grids is around 4%.

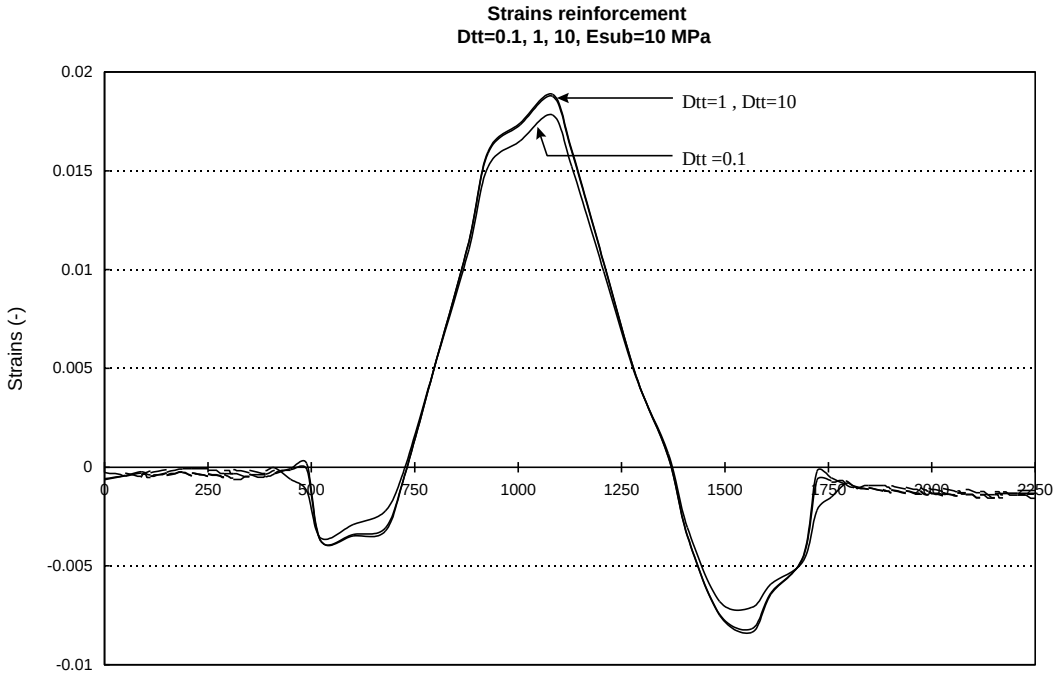

Figure 6.18 Strains in reinforcement as a function of D_{tt} for EA=5000 N/mm, subsoil 10 MPa

Figure 6.18 shows that the bond stiffness D_{tt} has a very small influence on the strains in the reinforcement. Between a bond of 1 and 10 N/mm/mm^2 there is no difference at all.

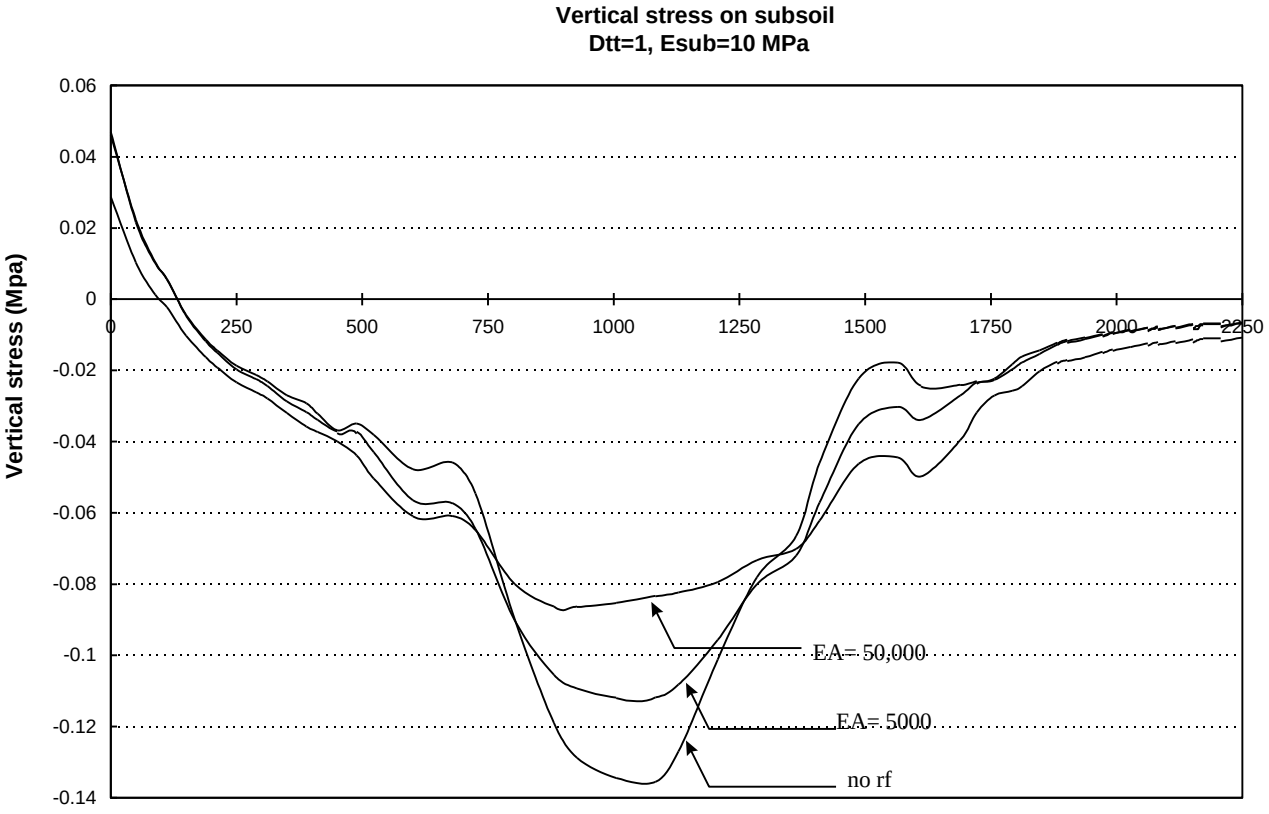

Figure 6.19 Vertical stresses on subsoil, 10 MPa subsoil

The stresses on top of the subsoil, figure 6.19, show a decrease when the structure is reinforced. The stiffer the reinforcement the bigger the decrease. This means that the vertical stress on the subsoil is relieved when the stiffness EA increases. Towards the left side of the structure (edge of the road) the direction of the stress is upwards due to bending.
The bearing capacity of the subsoil is determined with the simplified formula [lit 15]:

$$q_{subsoil}=5.14 \cdot f_{undr} \qquad (6.1)$$

where

$q_{subsoil}$	: bearing capacity of the subsoil	(kPa)
f_{undr}	: 30 ·CBR	(kPa)
E	: 10 CBR	(MPa)

With a maximum vertical stress of 135 kPa (for the not reinforced case) the bearing capacity of the subsoil being 154.2 kPa (5.14 ·30 ·1) is not exceeded. When a reinforcement is applied with an stiffness of 5000 N/mm the vertical stress on the subsoil reduces to approximately 115 kPa.

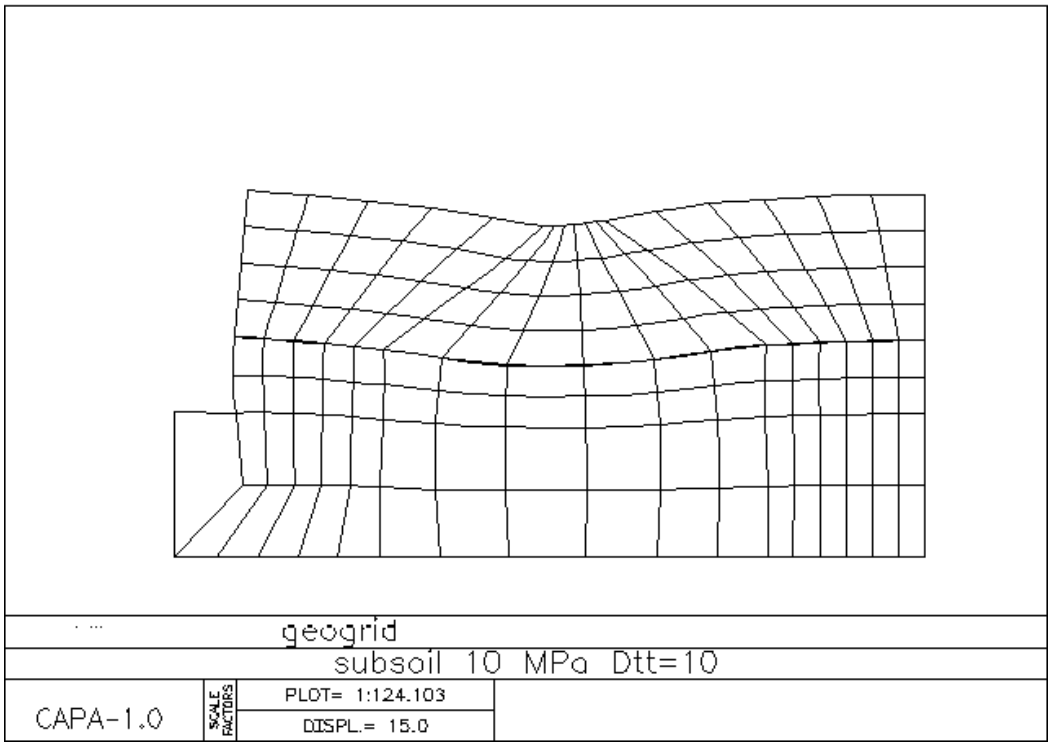

Figure 6.20 Deformed mesh, subsoil 10 MPa

In figure 6.20 the deformed mesh can be seen. The mesh shows that the left side of the road has expanded.
The influence on the displacements when different bond stiffnesses are used is very small, see figure 6.21. An improvement of only 2% is reached.

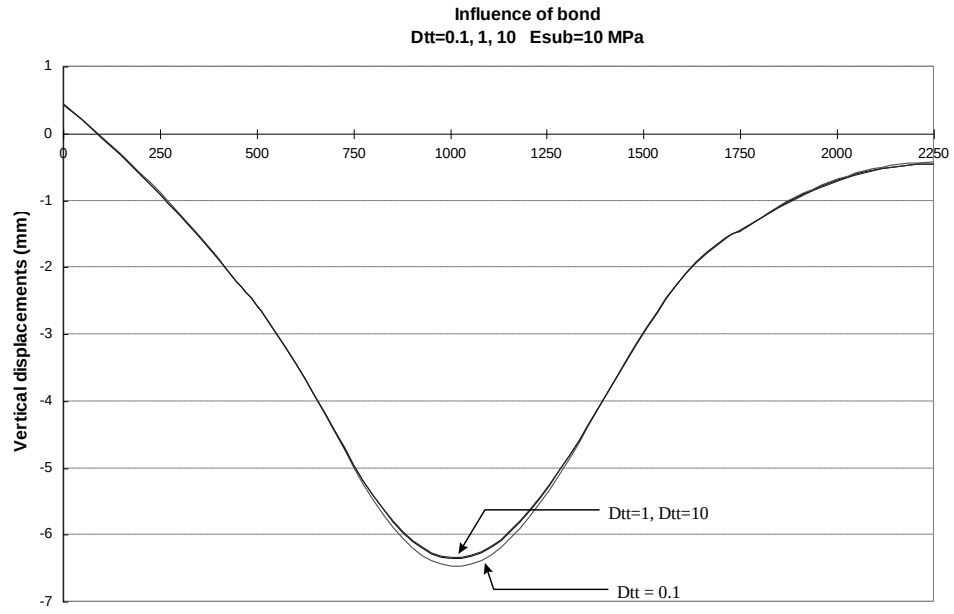

Figure 6.21 Influence bond on displacements (10 MPa subsoil)

The influence of the bond stiffness for the other cases can be seen in annex 3.4 till 3.6. It will come clear from the annex that the stiffer the reinforcement the bigger the influence on the displacements will be, when a higher bond stiffness is used. For the steel an improvement of approximately 8% is reached for the good bond (1 and 10 N/mm/mm^2) cases. Furthermore it can be concluded that there is no difference between 1 and 10 N/mm/mm^2 bond stiffness for the deflections.

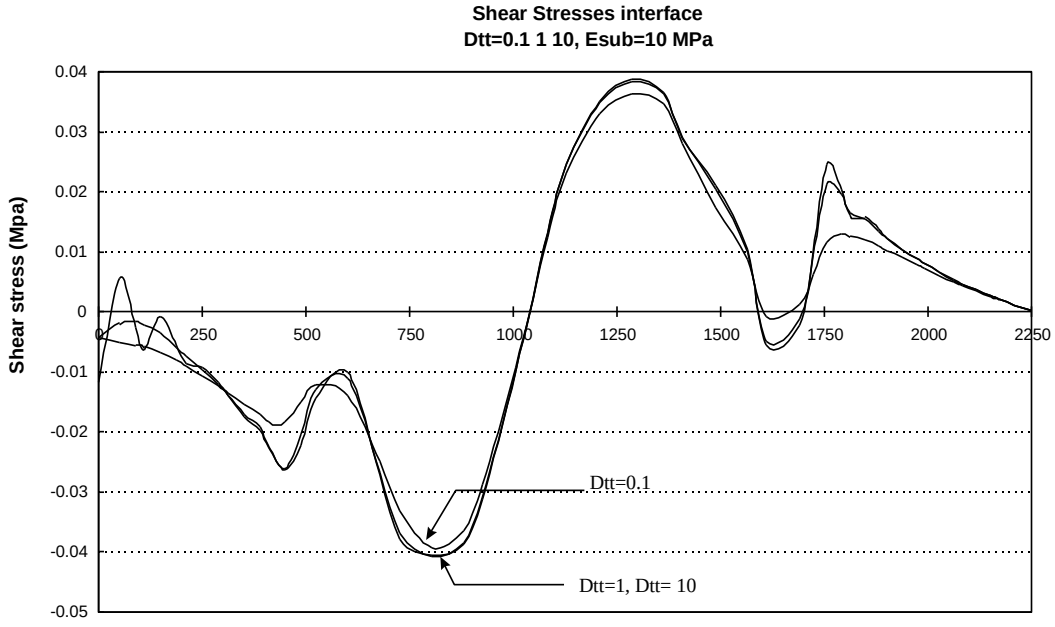

Figure 6.22 Influence of bond stiffness on shear stress interface (10 MPa subsoil)

Figure 6.22 shows that the influence of the shear stress in the interface is very small. Figure 6.23 gives a better idea what happens in the interface when different bond coefficients are considered. A bond stiffness of 10 N/mm/mm^2 shows a very small value for the shear stress.

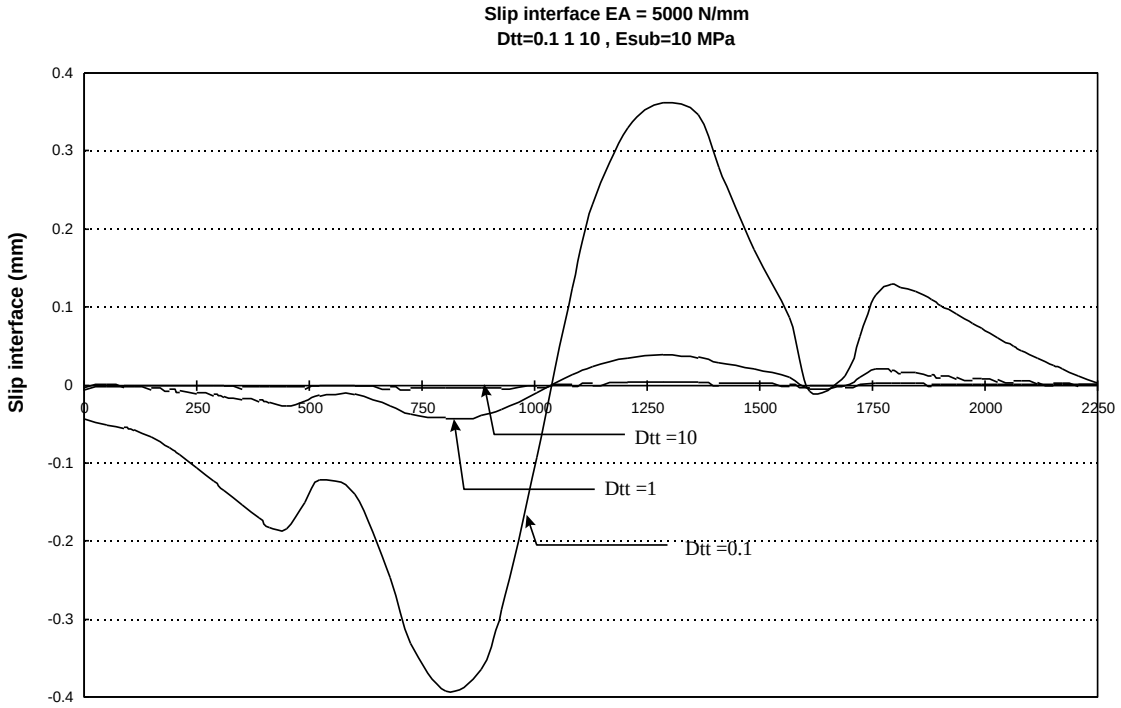

Figure 6.23 Influence bond stiffness on slip interface as a function of D_{tt} with EA = 5000N/mm

Figure 6.23 makes clear that the bond stiffness certainly has some influence. The bigger the bond stiffness, the lower the slip will be (horizontal displacement). When the bond stiffness is too low, it will be a possibility that the interface and therefor the reinforcement are pulled out.

6.6.2 Output for the 25 MPa subsoil

In this paragraph the influence on the displacements due to an increased subsoil stiffness (2.5 times bigger) and an increased base stiffness (1.8 times bigger) is shown.
Figure 6.24 shows that if the structure is made on an average 2.2 times stiffer the vertical displacements will decrease proportional.
The difference with the no reinforced case and the two reinforced cases regarding the displacements is 9% and 23% respectively.

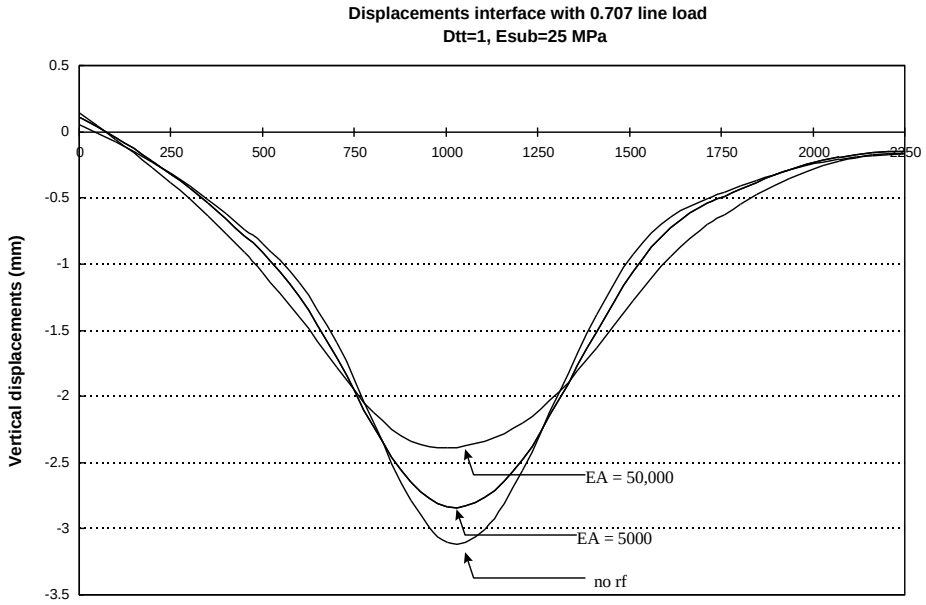

Figure 6.24 Vertical displacements at the interface, 25 MPa subsoil

Figure 6.25 shows the development of the strains for this case. Compared with the 10 MPa subsoil case the strains also show some decrease. This is logical because the displacements are smaller due to the better stiffness properties.

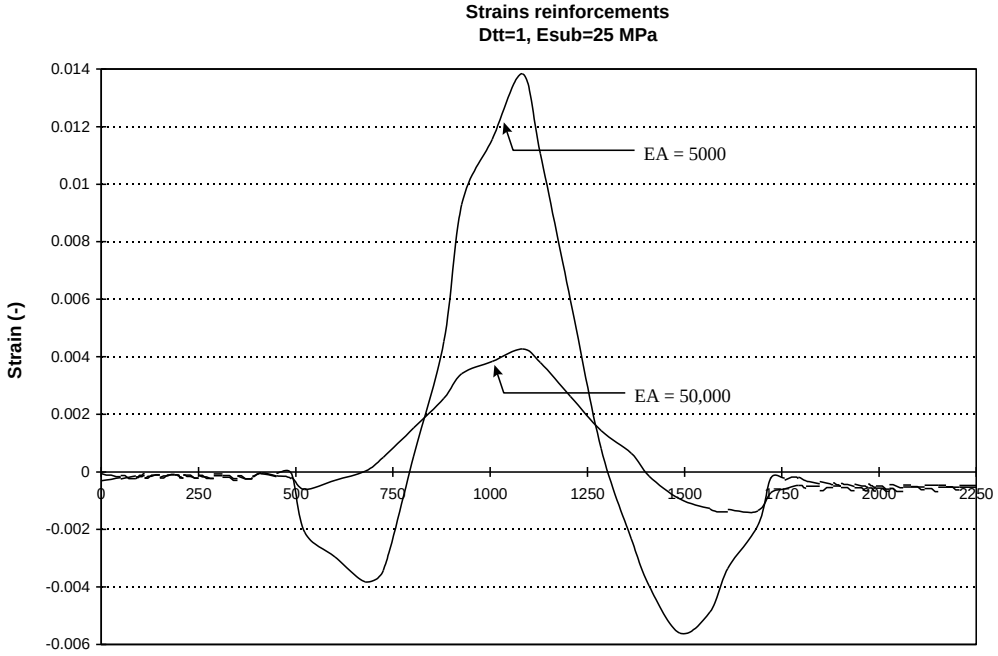

Figure 6.25 Strains in reinforcement as a function of EA for D_{tt}=1 N/mm, subsoil 25 MPa

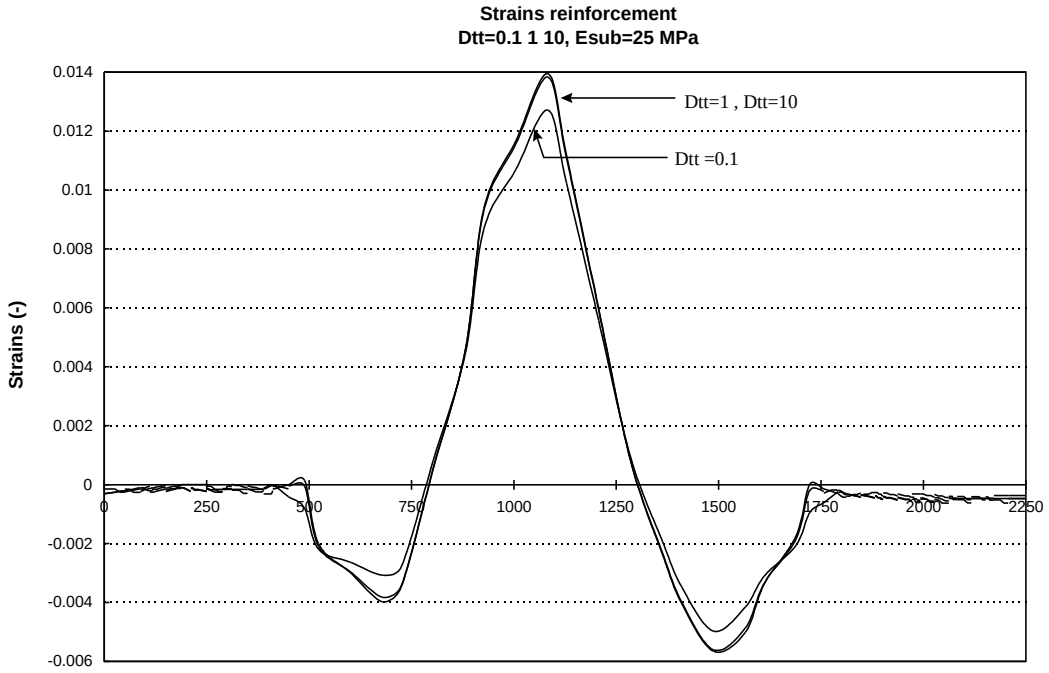

Figure 6.26 Strains in reinforcement as a function of D_{tt} for EA=5000 N/mm/mm^2, subsoil 25 MPa

Figure 6.26 has the same trend as the graph of figure 6.18, only are the values for the strains of this case somewhat smaller.

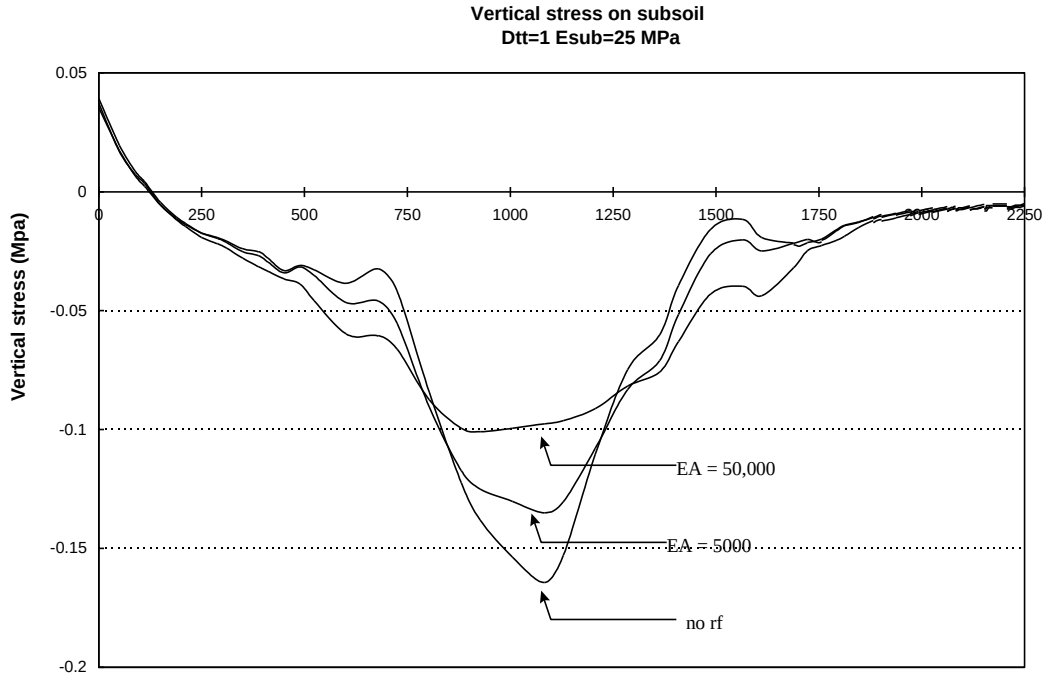

Figure 6.27 Vertical stresses on top of the subsoil (25 MPa)

Figure 6.27 shows that as the stiffness of the subsoil increases the vertical stresses on the subsoil will also increase.
The bearing capacity of the subsoil (6.1), $5.14 \cdot 30 \cdot 2.5 = 385.5$ kPa, is not exceed since the maximum stress on the subsoil is around 160 kPa

The deformed mesh in figure 6.28 shows that the displacements of the left boundary (edge of the road) are less compared with the 10 MPa case of figure 6.20.

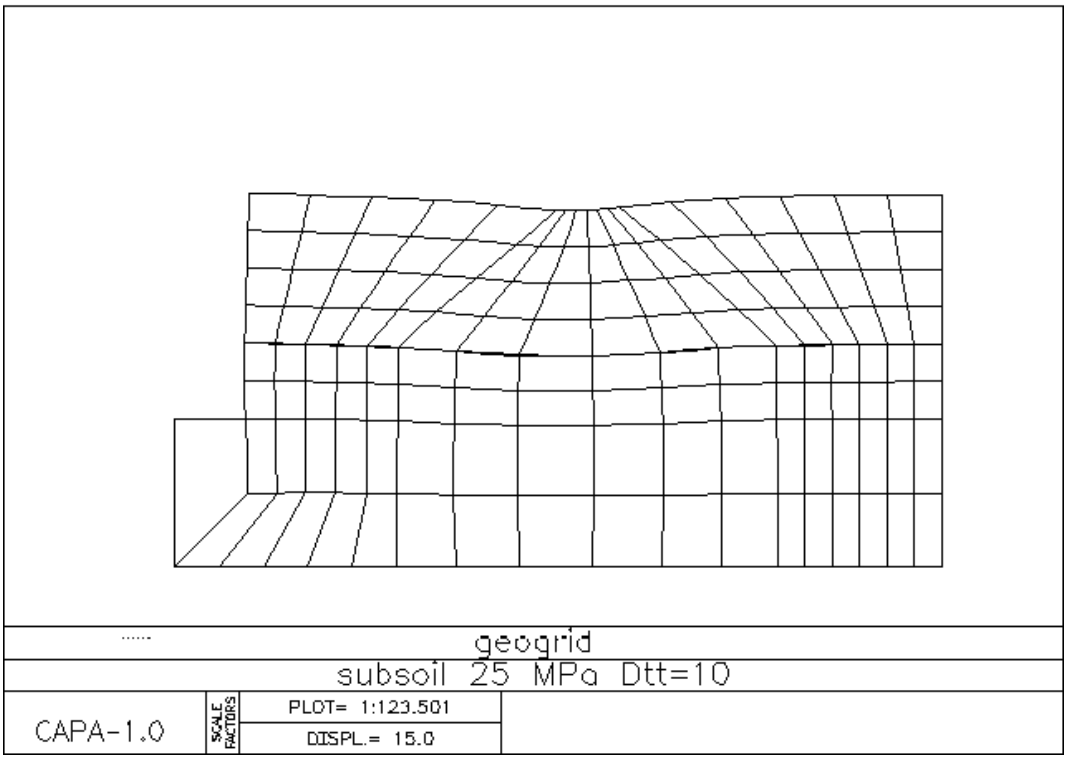

Figure 6.28 Deformed mesh, subsoil 25 MPa

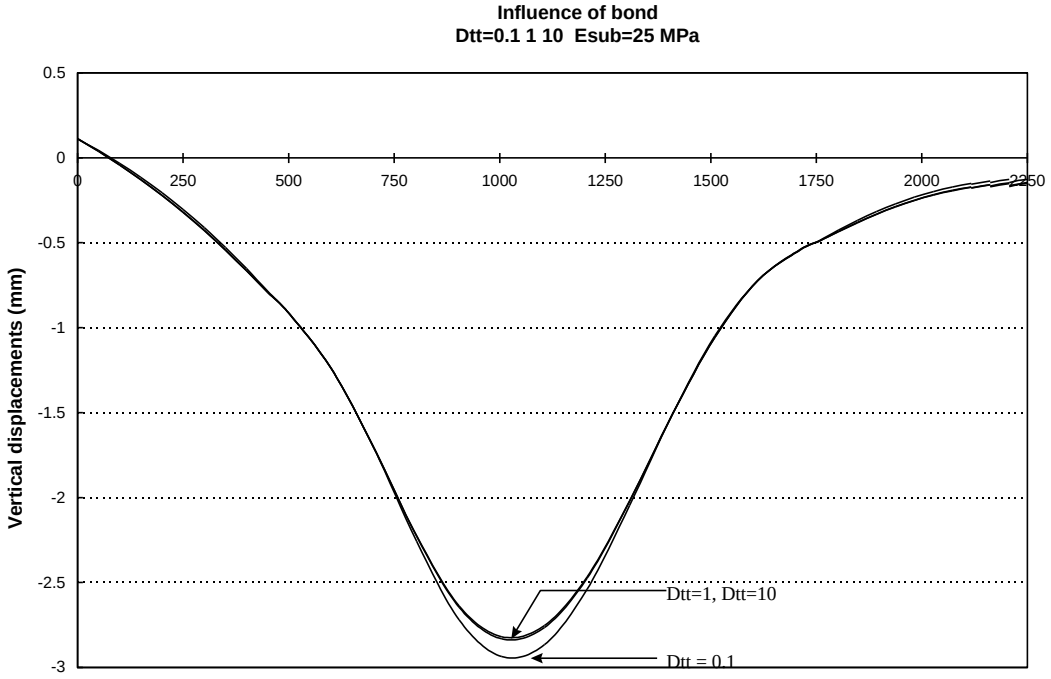

Figure 6.29 Influence of bond on vertical displacements (25 MPa subsoil)

From figure 6.29 it is also concluded that the influence of different bond stiffnesses on the vertical displacements is very marginal.
Between a bond of 1 and 10 N/mm/mm^2 there is no difference in displacements at all.

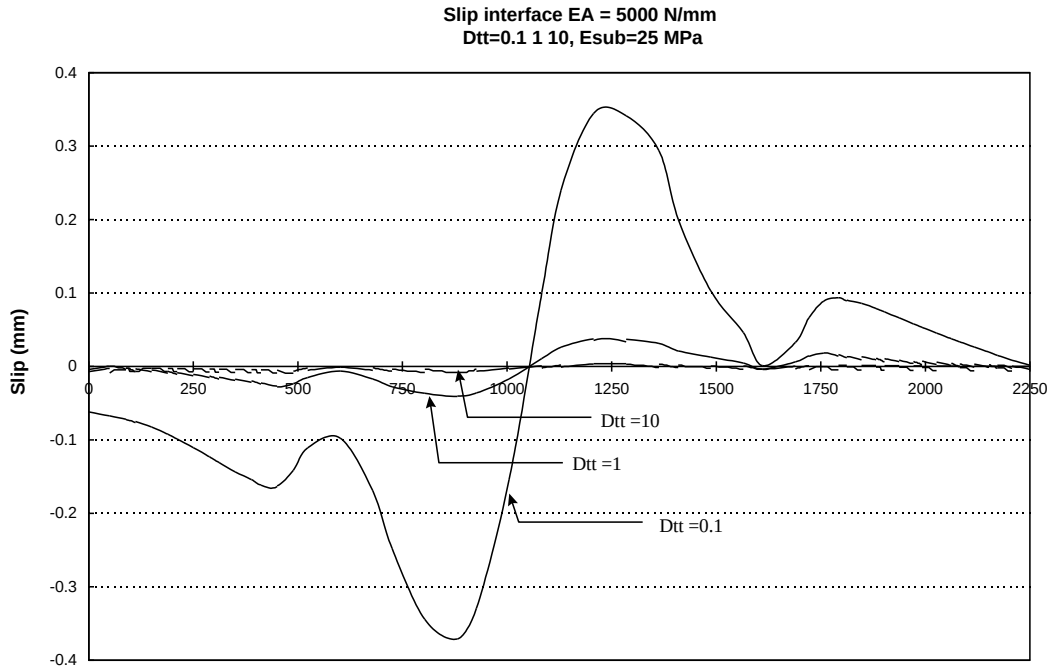

Figure 6.30 Influence bond stiffness on slip interface as a function of D_{tt} with EA = 5000N/mm

When figure 6.30 is compared with figure 6.23, the figure shows very little difference.

6.6.3 Output for the 50 MPa subsoil

In figure 6.31 the displacements are shown for the 50 MPa case. When the stiffness properties are further increased with a factor of 1.75 on average the displacements decrease proportional. The improvement with reinforcement is 8% for EA=5,000 N/mm and 23% for EA=50,000 N/mm.

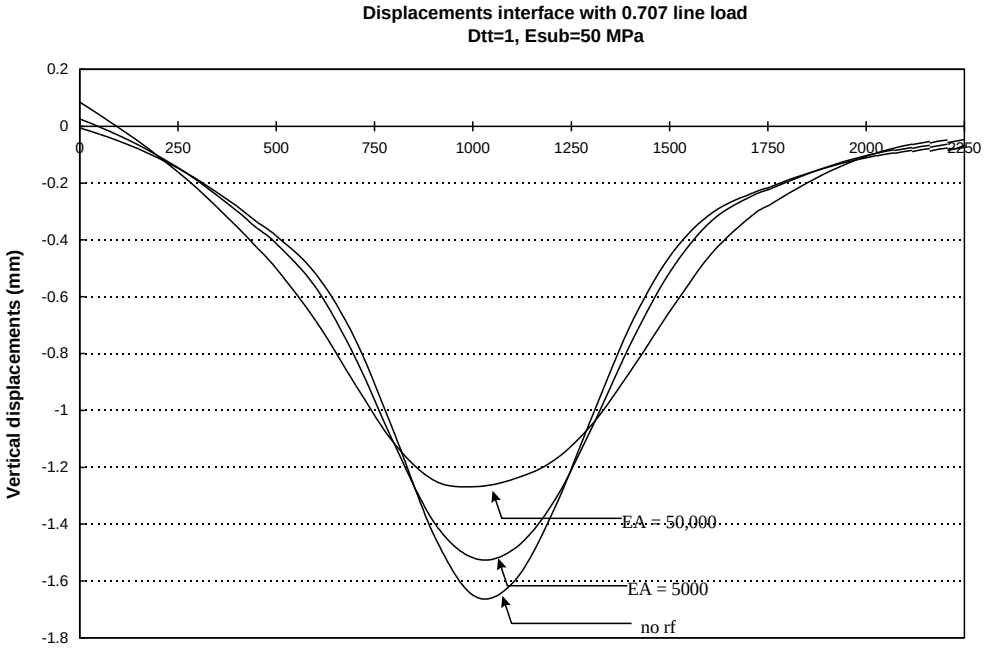

Figure 6.31 Vertical displacements at the interface, subsoil 50 MPa

When figure 6.32 is considered one can see that for the stiff reinforcement (EA=50,000 N/mm) the maximum strain is 0.4% and for the weaker reinforcement (EA=5000 N/mm) the maximum strain is about 1.2%.

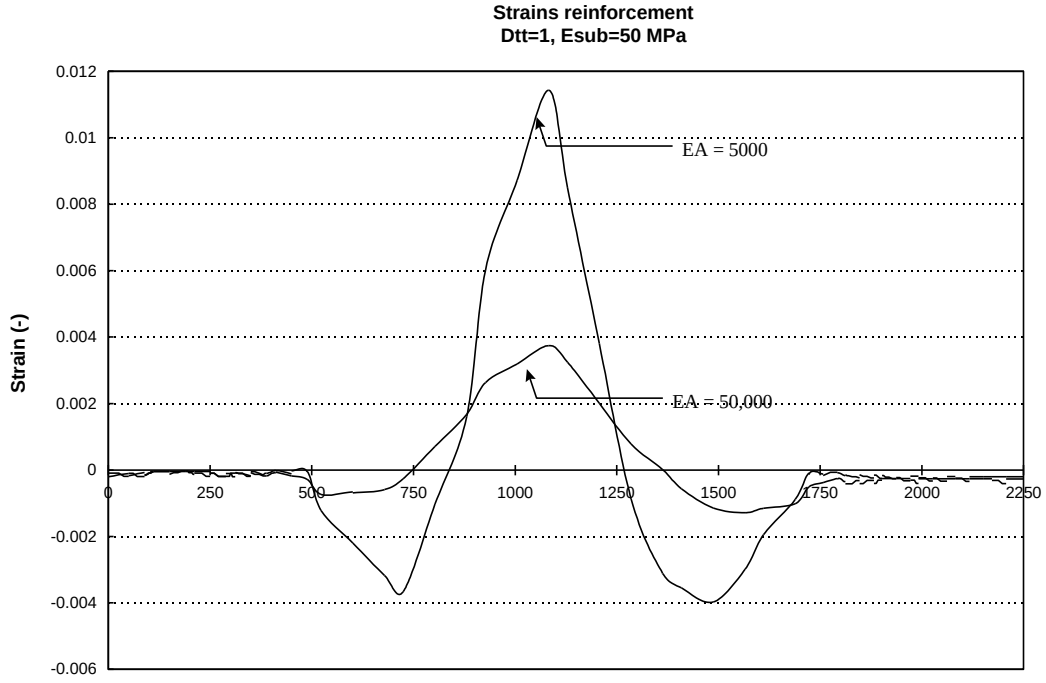

Figure 6.32 Strains in reinforcement as a function of EA for D_{tt}=1 N/mm, subsoil 50 MPa

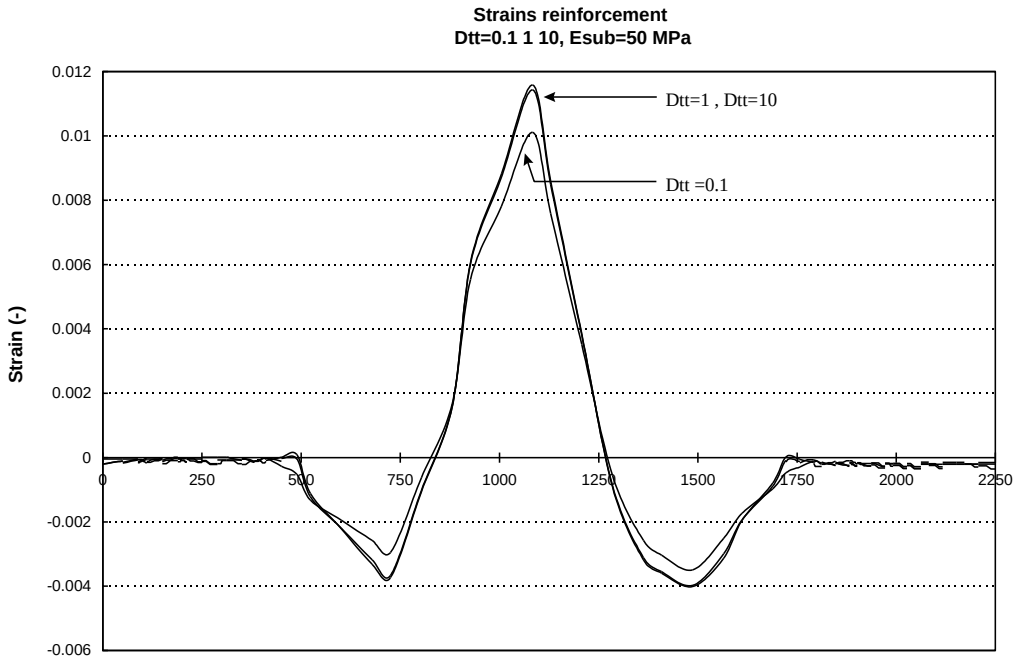

Figure 6.33 Strains in reinforcement as a function of D_{tt} for EA=5000 N/mm, subsoil 50 MPa

The stiffer the structure (base and subsoil) the lower the strains in the reinforcement will be, figure 6.33.

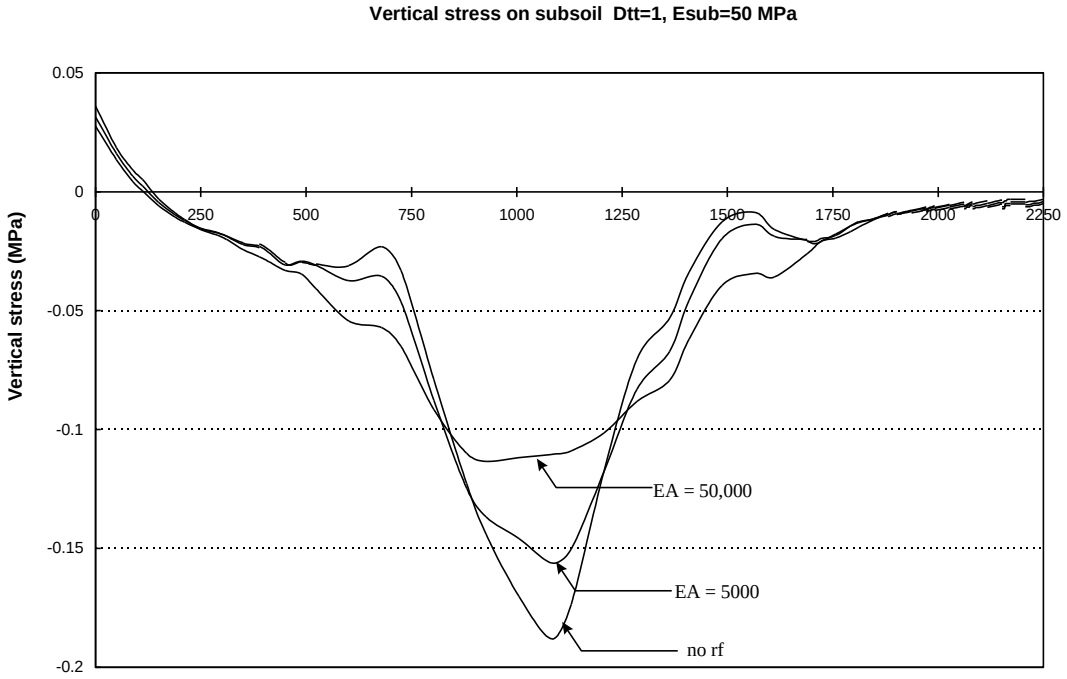

Figure 6.34 Vertical stresses on subsoil, 50 MPa subsoil

Figure 6.34 shows that when the stiffness of the subsoil increases furthermore the stresses on the subsoil will also increase.
The bearing capacity of the subsoil is for this case $5.14 \cdot 30 \cdot 5 = 771$ kPa.

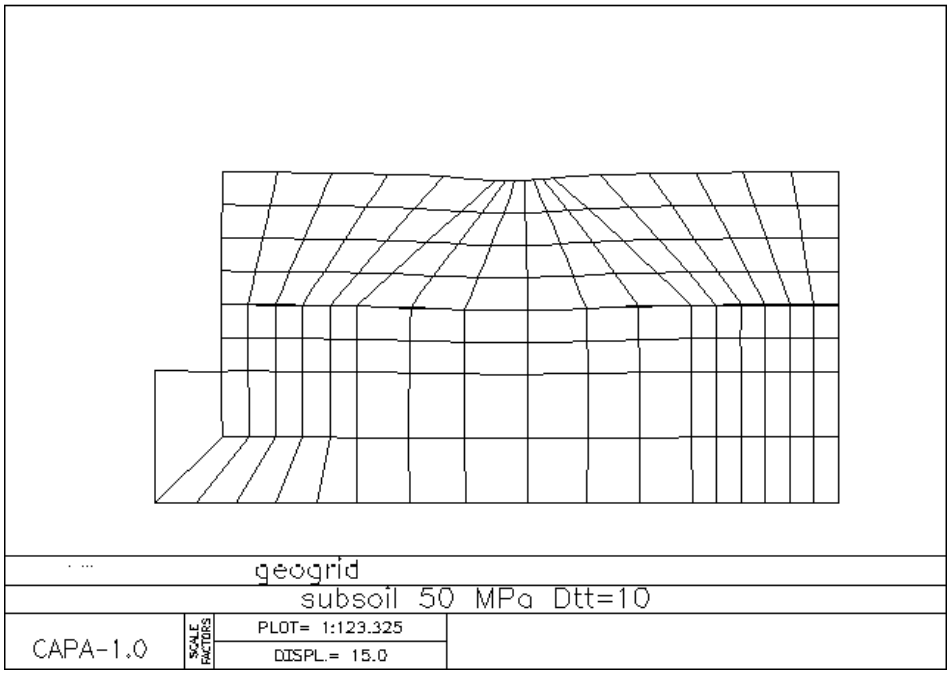

Figure 6.35 Deformed mesh, subsoil 50 MPa

Figure 6.35 shows the deformed mesh for this case. The figure makes clear that the left boundary shows almost no displacement in the x direction.

Figure 6.36 shows that the influence on the displacements when different bond stiffnesses are being used is bigger (approximately 7%). This is because the anchoring of the interface is better due to the higher elastic moduli of the base and of the subsoil.
The figure shows furthermore that a bigger bond stiffness gives no improvement, the displacements for a bond of 1 and 10 N/mm/mm^2 are the same.

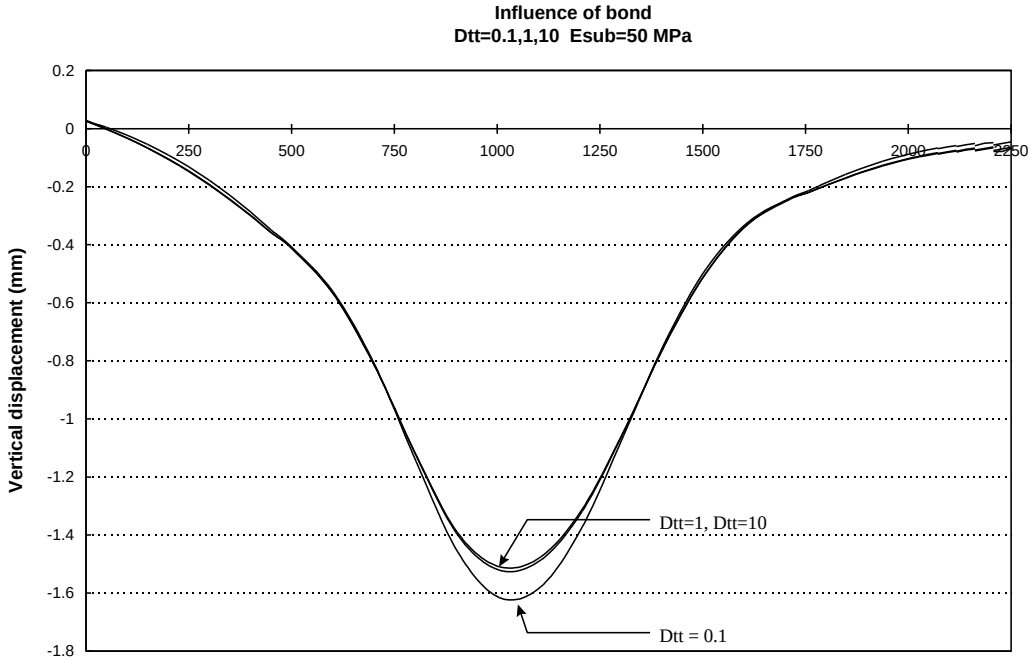

Figure 6.36 Influence of bond on vertical displacements (50 MPa subsoil)

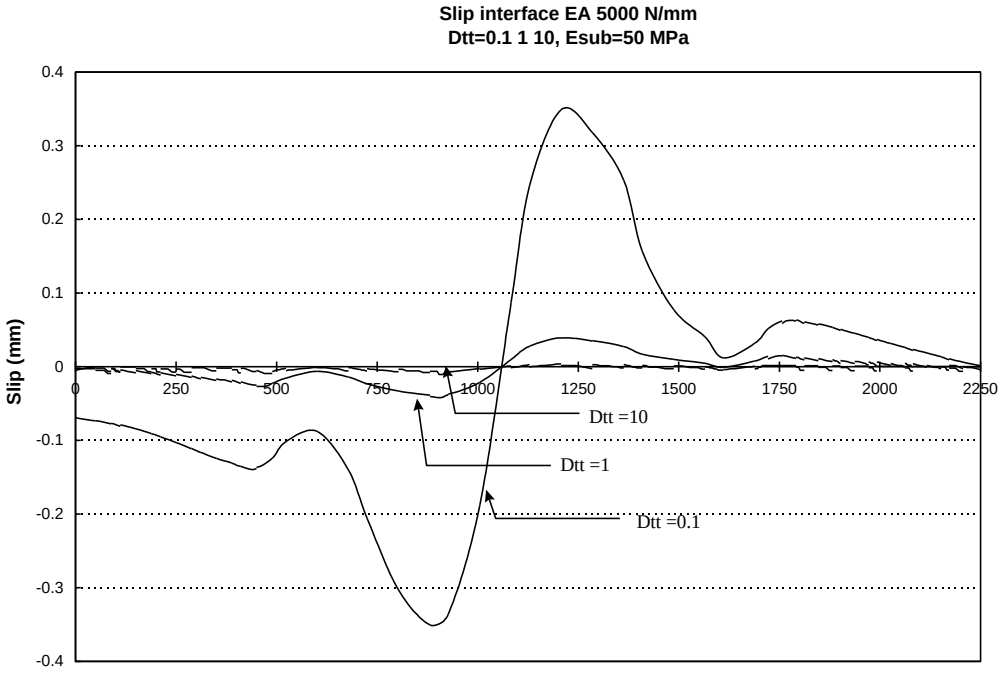

Figure 6.37 Influence bond stiffness on slip interface as a function of D_{tt} with EA = 5000N/mm

Figure 6.37 shows the slip of the interface as a function of D_{tt} for this case. The curves for the slip are for all the cases (with the different subsoils) of the same magnitude.

6.7 Parameter study for the 350 mm base

6.7.1 Output for the 25 MPa subsoil

In this paragraph the results for the 350 mm thick base are presented and discussed. Because of the decreased base thickness the load on the interface will be bigger. This immediately results in bigger vertical displacements of the interface material. Figure 6.38 shows this (compare with figure 6.24). The improvement regarding the displacement is 7% and for the stiffer reinforcement 20%.

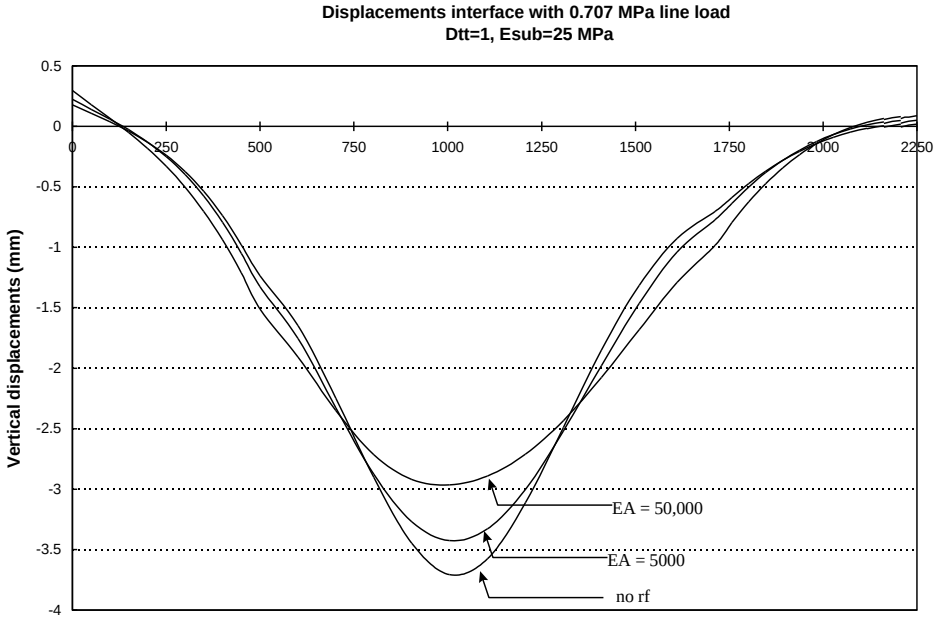

Figure 6.38 Vertical displacements at the interface, subsoil 25 MPa

Figure 6.39 shows the strains for this case. The figure shows that the difference between the 500 mm and the 350 mm case (figure 6.25) is very small. They are both of the same magnitude.

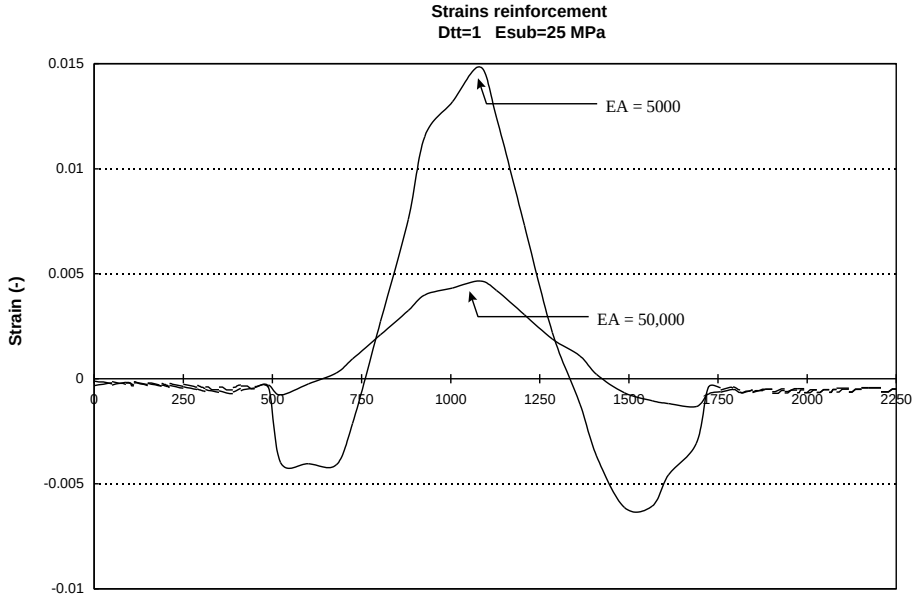

Figure 6.39 Strains in reinforcement as a function of EA for D_{tt}=1 N/mm, subsoil 25 MPa

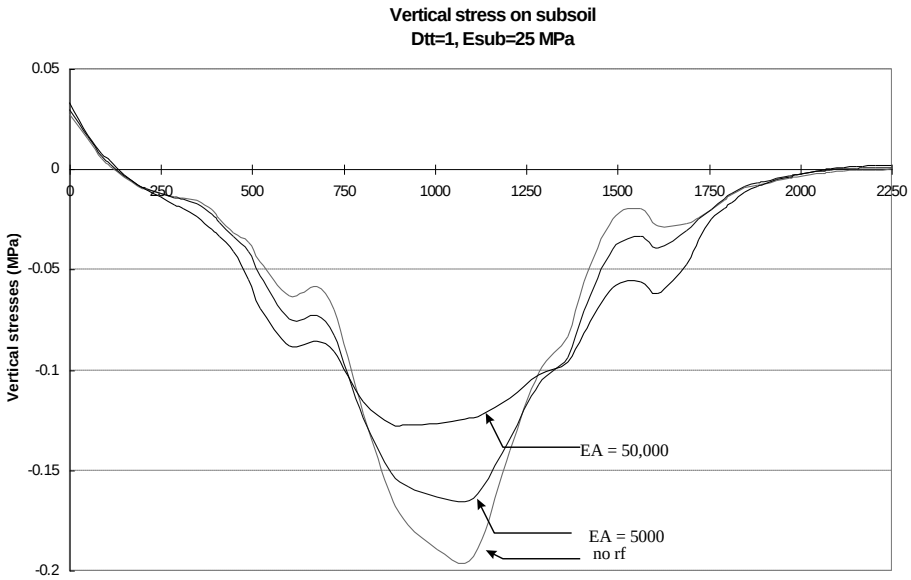

Figure 6.40 Vertical stresses on subsoil, 25 MPa subsoil

Figure 6.40, the vertical stress on the subsoil shows that when the base thickness decreases the vertical stress increases. The bearing capacity of the subsoil (385.5 kPa) is not exceeded.

Figure 6.41 shows the deformed mesh.

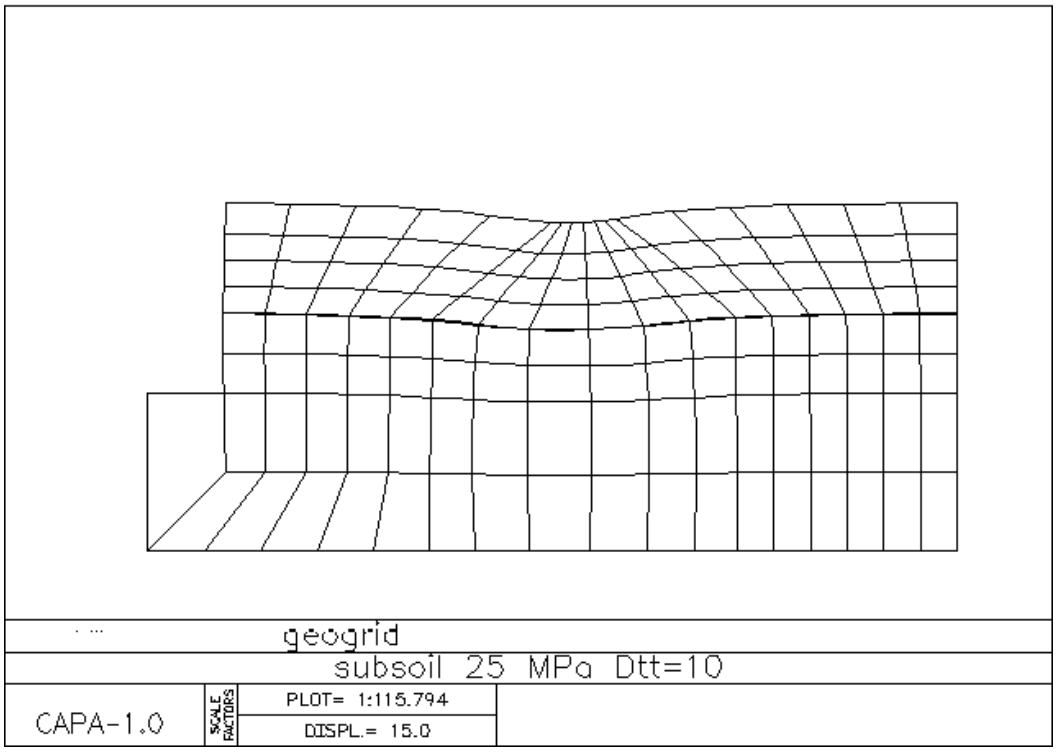

Figure 6.41 Deformed mesh, subsoil 25 MPa

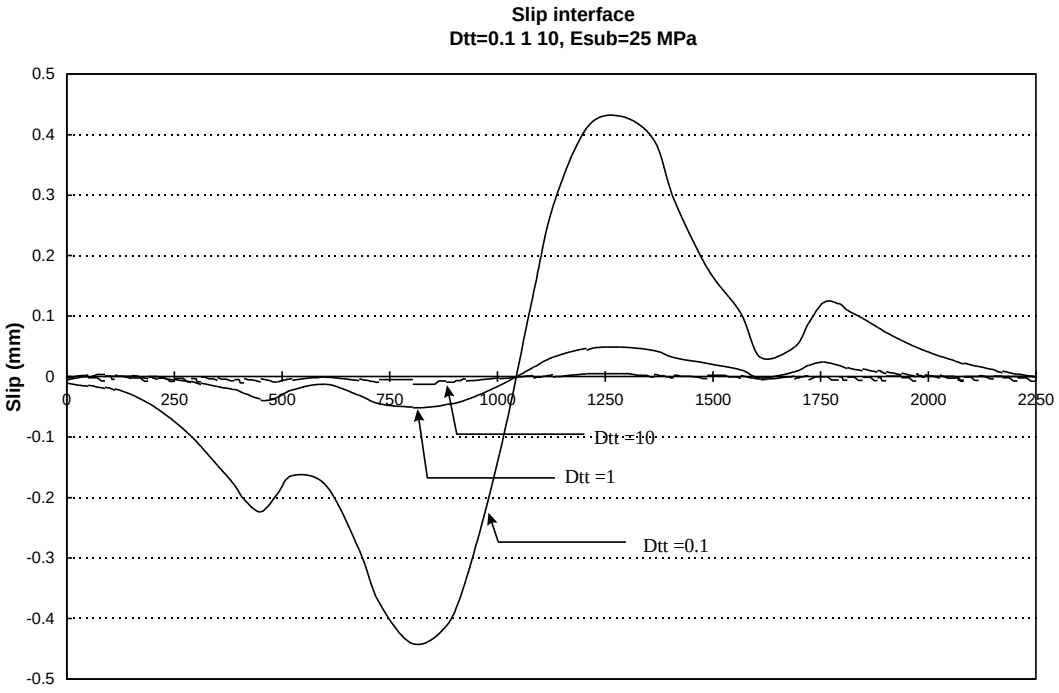

Figure 6.42 Influence bond stiffness on slip interface as a function of D_{tt} with EA = 5000N/mm

Figure 6.42 the graph presenting the influence of the bond stiffness on the slip is of the same magnitude as the other cases.

6.7.2 Output for the 50 MPa subsoil

When the stiffness is increased with a factor of 1.88 the displacements will decrease proportional. The maximum displacement for the 25 MPa case is 3.71 mm. (figure 6.43) and for the 50 MPa case it is 2.04 mm. The decrease therefore is 1.69 mm.
The improvement (using a stiffer grid) is 7% and 20% respectively.

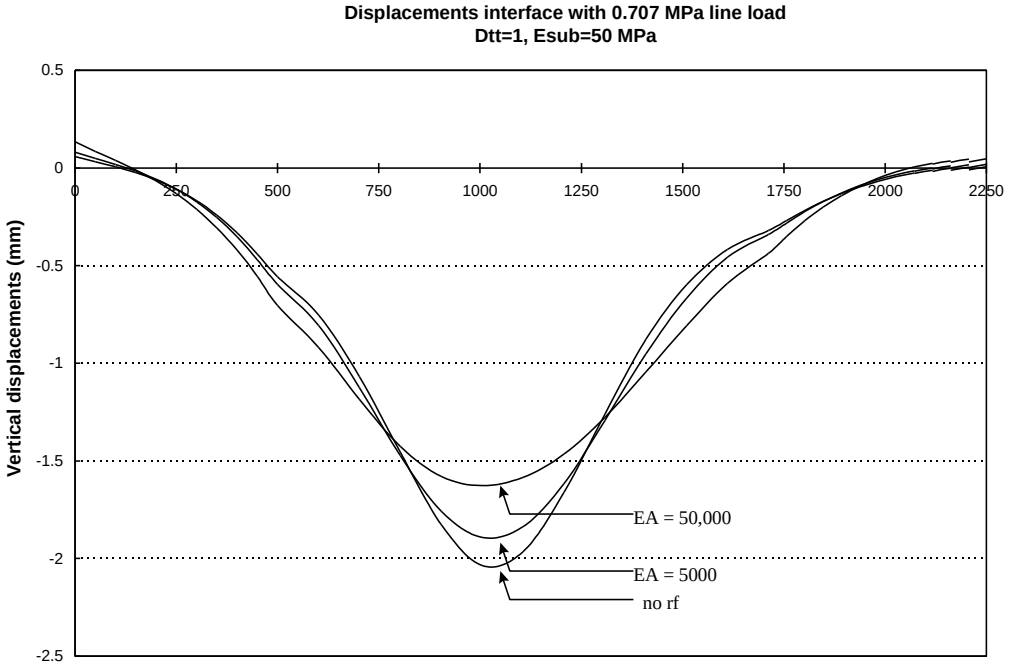

Figure 6.43 Vertical displacements at the interface, subsoil 50 MPa

Figure 6.44 shows that the strains have decreased due to the stiffer properties of the subsoil and the base.

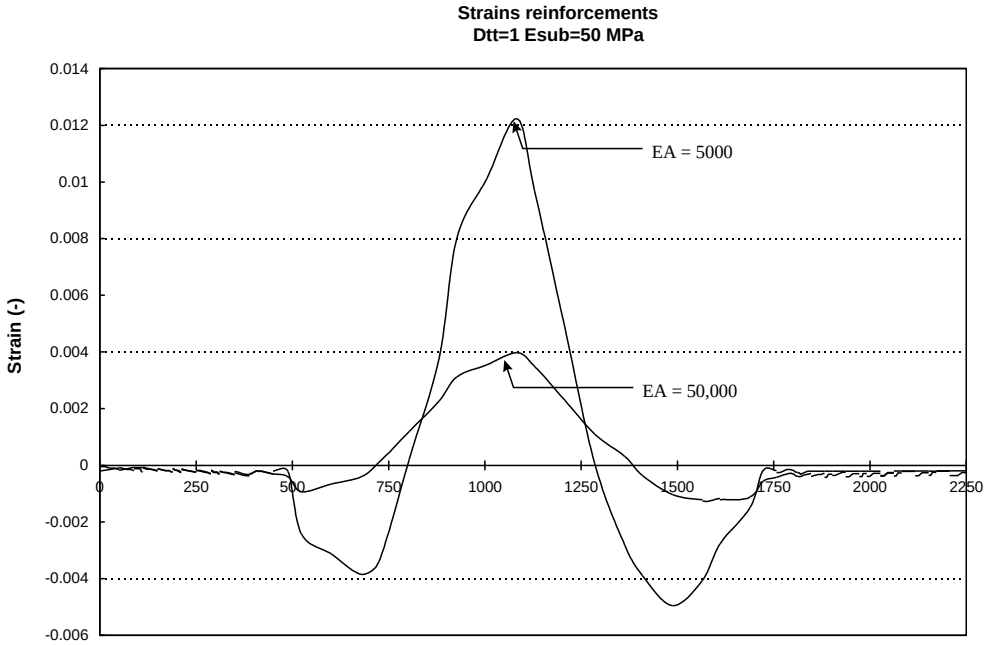

Figure 6.44 Strains in reinforcement as a function of EA for D_{tt}=1 N/mm, subsoil 50 MPa

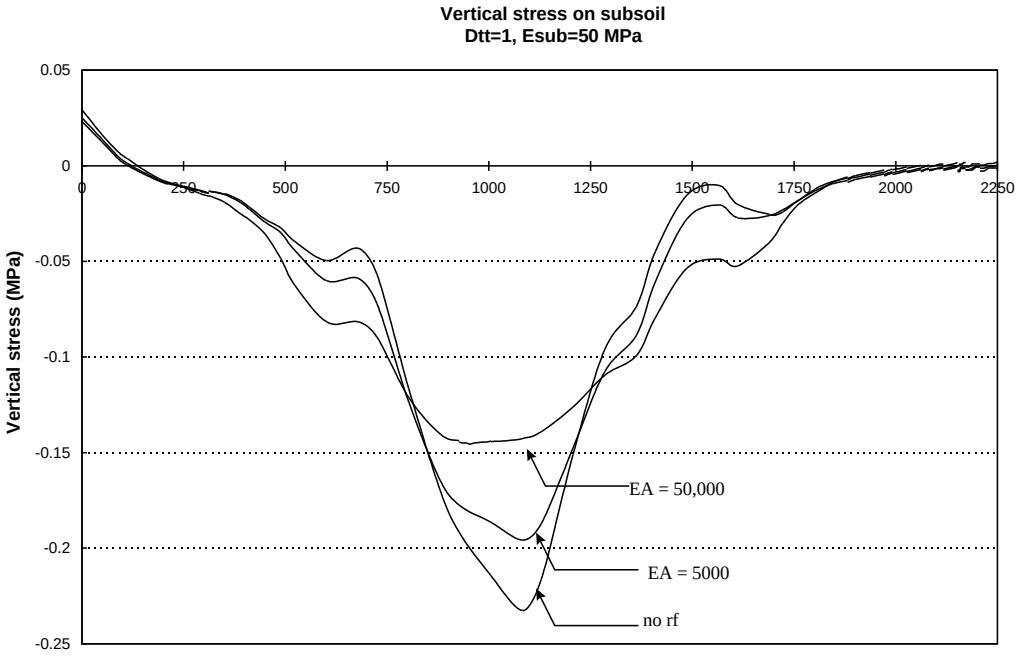

Figure 6.45 Vertical stresses on subsoil, 50 MPa subsoil

Figure 6.45 shows the vertical stress on the subsoil. The maximum vertical stress is 230 kPa. The bearing capacity of the subsoil has not been exceeded.

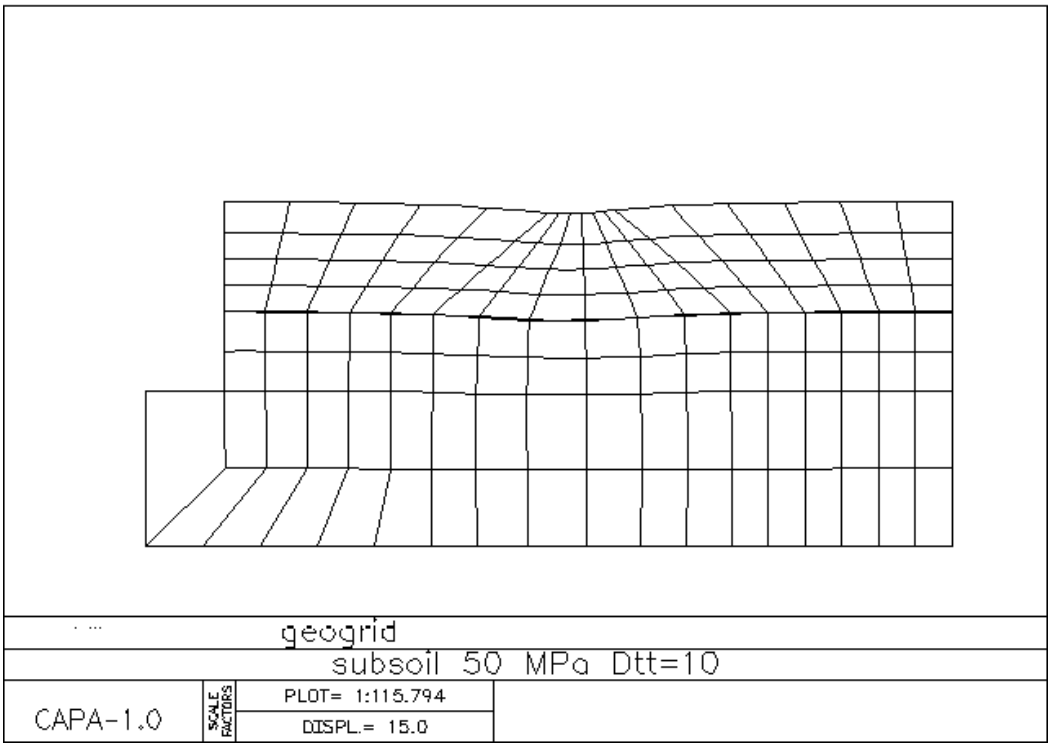

Figure 6.46 Deformed mesh, subsoil 50 MPa

Figure 6.46 shows the deformed mesh. The movement to the left side is decreased compared with the 25 MPa case of figure 6.41.

Figure 6.47 shows the slip of the interface which is of the same magnitude as the previous case with a subsoil stiffness of 25 MPa.

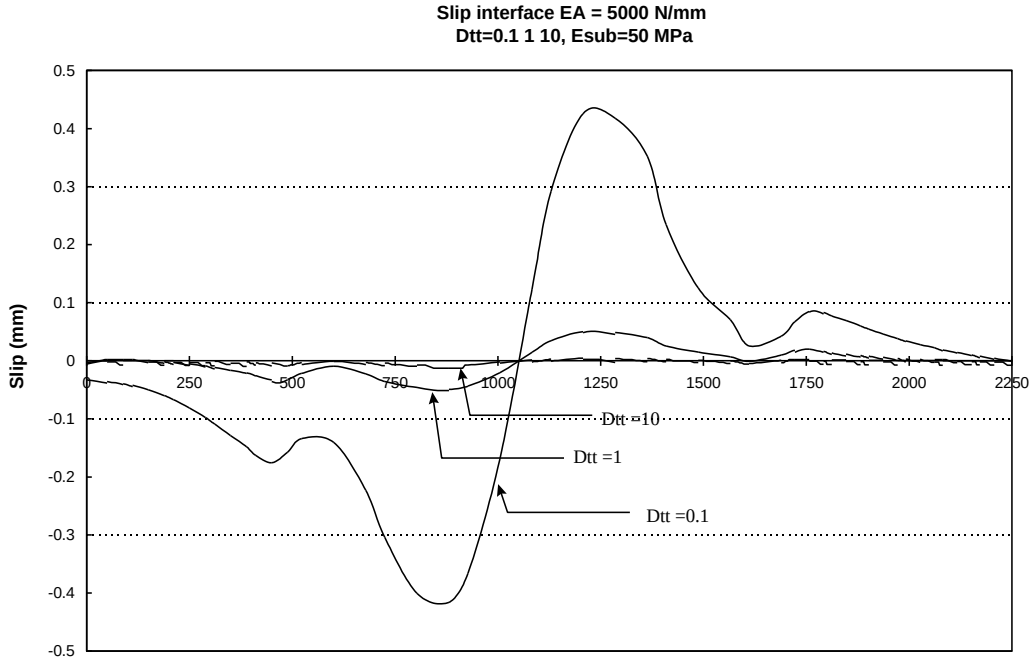

Figure 6.47 Influence bond stiffness on slip interface as a function of D_{tt} with EA = 5000N/mm

6.8 Concluding graphs

In this paragraph the overall output for all the cases is presented. The maximum values are plotted for different stiffnesses of the reinforcement and different subsoil stiffnesses. Figure 6.48 shows the maximum values for the displacements, figure 6.49 the maximum values for the vertical stresses on the subsoil and figure 6.50 shows the maximum values for the slip of the interface. The graphs are plotted on a logarithmic scale.

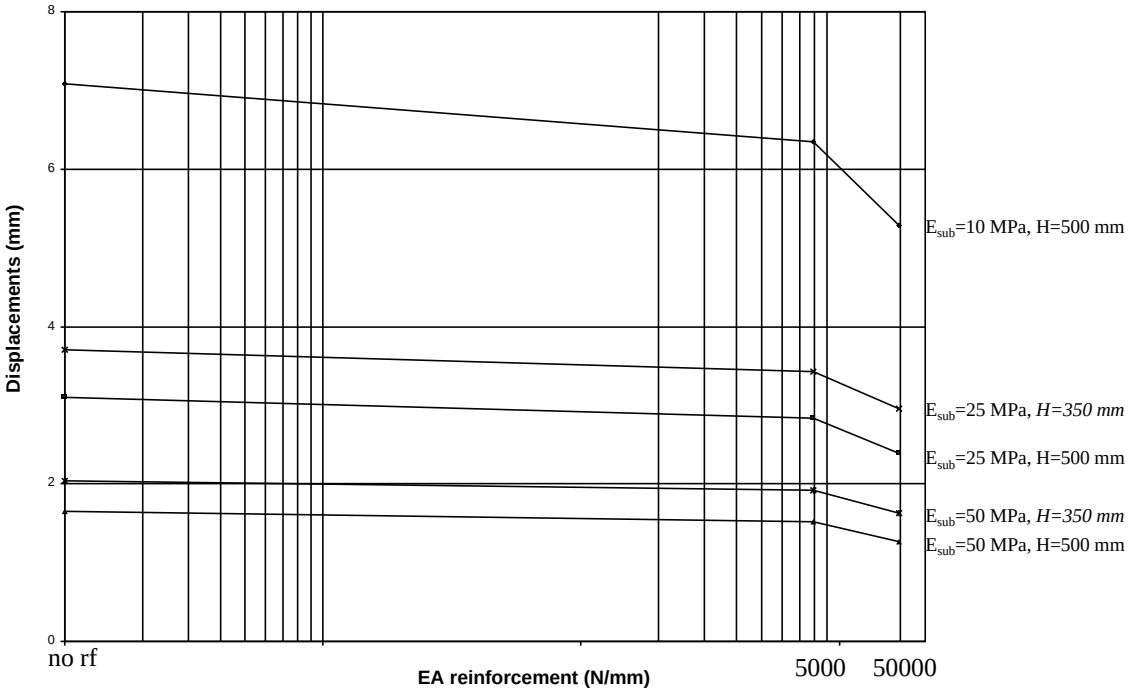

Figure 6.48 Vertical displacements as a function of EA and subsoil stiffness

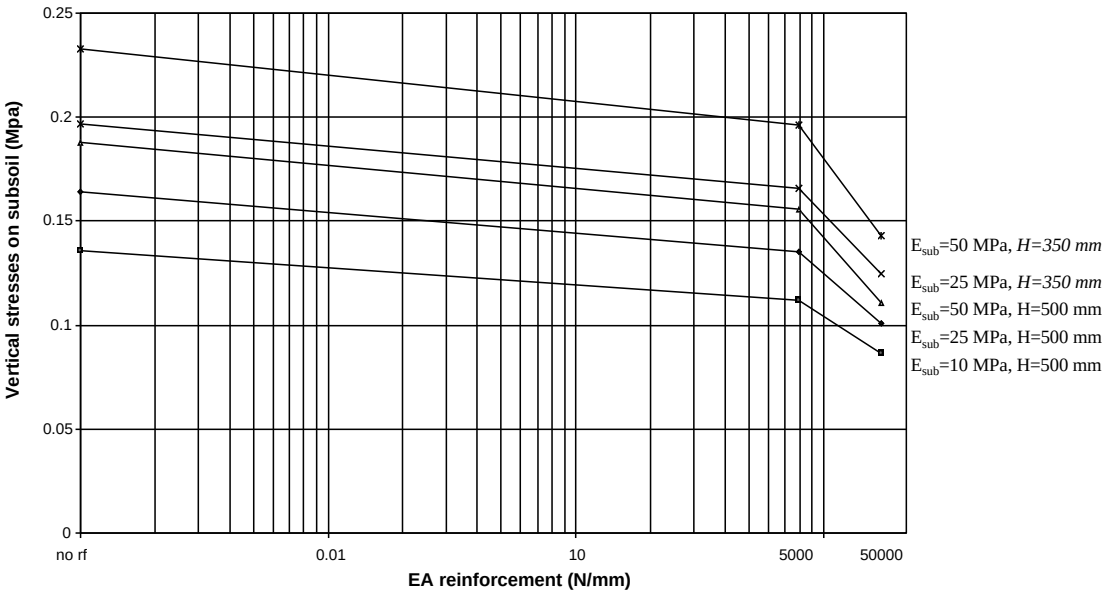

Figure 6.49 Vertical stress on subsoil

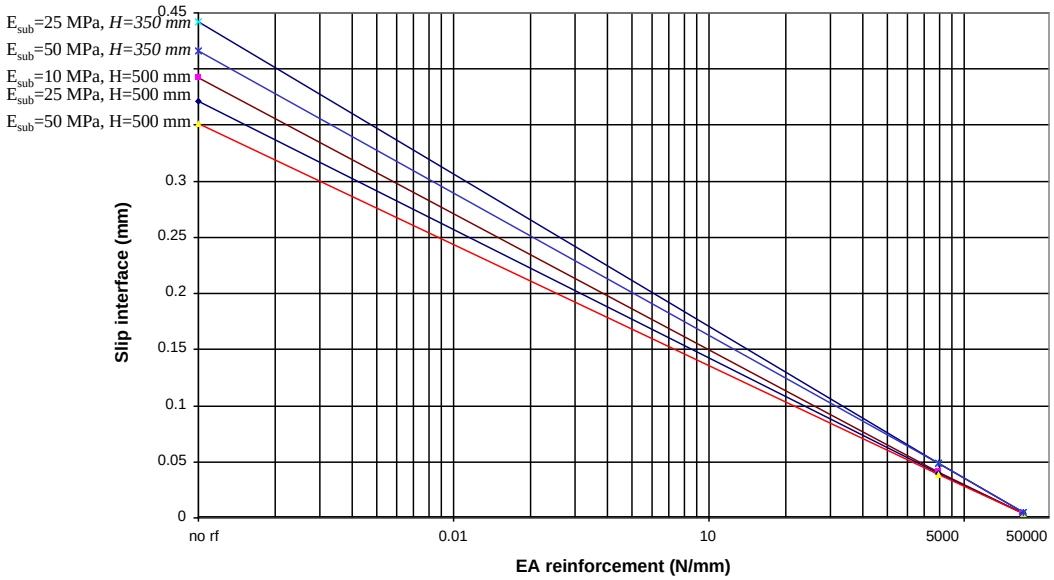

Figure 6.50 Slip interface

6.9 Conclusions

- The main parameters of influence are the bond stiffness, the stiffness of the reinforcement and the stiffness of the subsoil and the thickness and the stiffness of the base material.
- The bond stiffness should not be confused with the Coefficient Of Interaction, the COI.
- Bond is strongly dependent on the effective normal stress, the size of the grids, the stiffness of the junctions and the shape of the aggregate.
- When the structure is completely isotropic ($E_{xx}=E_{yy}$) there is hardly any influence on the displacements, if the reinforced case is compared with the not reinforced case.
- When the structure is partly anisotropic in those areas where tensile stresses most likely will occur ($E_{xx}\rightarrow 0$) the usage of the reinforcement will become effective by decreased displacements of the structure.
- When the complete structure assumed to be anisotropic ($E_{xx}=0$) the forces can't be transmitted into the reinforced area anymore.
- The vertical displacements reduce with approximately 10% when a reinforcement with an EA of 5,000 N/mm is used and with approximately 25% when a reinforcement with an EA of 50,000 N/mm is used.
- The vertical stresses on the subsoil reduce when a reinforcement is used. In all analyzed cases the subsoil can bear this vertical stress.
- The 4 sublayers of the base can be replaced with only 2 sublayers, the displacements are the same for both cases.
- When the stiffness of the interface increases (the D_{tt}), the displacements won't decrease proportional.
- When the interface stiffness, D_{tt}, increases, the slip of the interface decreases. The risk of the reinforcement to be pulled out will be reduced.
- The further from the loaded area, the smaller the D_{tt} ought to be, because of the smaller (normal) stresses. In the calculations however one average bond stiffness is used for the whole width of the road.
- When the base is made thinner, the displacements are bigger due to the higher stresses on the interface and the subgrade.
- An unreinforced base of 500 mm gives more or less the same displacements as a 350 mm reinforced base with an EA of 50,000 N/mm, this means that if a reinforcement is used the base thickness can be reduced (in this survey a reduction of 30% is reached with the stiffest reinforcement).
- For an optimal force transmission into the reinforcement the bond between reinforcement and aggregate should be good.
- The influence on the displacements will be less when low bond and poor soil properties are used compared with good bond and soil properties.
- The influence of the bond is bigger as the stiffness of the reinforcement increases.
- Above a certain value (say 1 $N/mm/mm^2$) the bond will show no improvement anymore for the displacements.
- The stresses/strains in the reinforcement follow the shape of the base. The reinforcement will be in tension under the loaded area and in compression towards the sides of the road (according to the bending theory).

7. Conclusions and recommendations

7.1 Conclusions

- The whole system of pavement modelling, material modelling, weak pavement structures and heavy loads is damned complicated.
- The common models and programs such as the program Kenlayer and the M_r-σ_3-σ_1 material model are, because of the weak subsoil properties and the heavy loads, not suitable to determine the base stiffness.
- Base reinforcement has a positive influence on the overall behaviour of the structure.
- The stiffer the subsoil, the lower the vertical displacements. In practice, the vertical displacement will be bigger, due to the increase of the water-stress when a vehicle is passing, which on its term will lead to an increase of the particle-stress of the soil and thus a lower subsoil stiffness. Furthermore will permanent deformations also lead to an increase of the vertical displacements of the structure.
- The value for the optimal bond stiffness and the value for the optimal grid stiffness must be feasible.

Detailed conclusions

- With engineering judgement material modelling (here determining the base stiffness) is still possible.
- Whatever material model is used, the output of the calculations of that model should be analyzed critically and objectively.
- When the stiffness parameters of the structure are assumed to be isotropic, meaning the elastic moduli having the same value in all directions ($E_{xx}=E_{yy}$), reinforcing the base won't be of use (no effect on the displacements).
- Anisotropic stiffness properties of the base (meaning $E_{xx}\rightarrow 0$) in those areas where tension is likely to occur, lead to a decrease in the displacements at the interface and a decrease of the vertical stresses on top of the subsoil. The reinforcement is activated.
- When the stiffness of the base and/or the subsoil increases, the displacements will decrease proportional, but an increase of the stiffness of the reinforcement won't lead to a proportional decrease of the displacements.
- In relation to the stiffness of the base, the stiffness of the subsoil and the bond stiffness of the interface, the stiffness of the reinforcement EA should have a certain value before it becomes effective. Far below this value reinforcing won't be of influence and above a certain value reinforcing won't show any improvement of the structure anymore.

- The displacements reduce with approximately 10% when a reinforcement with an EA of 5,000 N/mm is used and with approximately 25% when an EA of 50,000 N/mm is used.

- The use of reinforcement has also a positive influence on the vertical stress on the subsoil. As the stiffness of the reinforcement increases the vertical stress on top of the subsoil decreases. However the bearing capacity of the subsoil is not normative for the cases analyzed here.

- The use of different bond stiffnesses D_{tt} has minor influence on the vertical displacement. The influence of the bond stiffness D_{tt} on the slip is bigger when it increases.

- When a reinforcement is used the base thickness can be reduced.

An unreinforced base of 500 mm gives more or less the same displacements as a 350 mm reinforced base with a reinforcement stiffness EA of 50,000 N/mm. This means a base reduction of 30% can be achieved.

- The design of this kinds of roads can be done using CAPA 2 D. But a few justifications (such as the use of anisotropic stiffness properties for the right super elements.) are needed.

These justifications are in favor compared with the disadvantages of the other design methods (such as the models of Sellmeijer and Houlsby):

- Houlsby omits the stiffness of the base totally (he looks only at the failure of the subsoil).
- Sellmeijer confuses material parameters with physical parameters.
- It is unclear what is done with E_{xx}, the horizontal stiffness of the base material.
- Sellmeijer has as starting point the cable theory. CAPA transforms the “cable” into a new layer and makes use of the bending theory.

7.2 Recommendations

- More investigation of the subsoil stiffness under a moving load.
- Three dimensional, non linear investigation. Allow permanent deformations.
- Investigation whether the optimum bond stiffness and the optimum grid stiffness are feasible.
- Determine the base stiffness for the cases where no or less tension can occur. This can be done with CAPA 2D for example.
- Determine the stiffness of the base also using a reinforcement.
- Introduce a (thin) asphalt layer, this because of the high stresses within the base. The stresses in the base will then be reduced.
- Investigation of the development of the tension stresses in the base.
- Determine whether the used stress distribution factor of 45^0 for the cases with reinforcement is justified.
- Try to introduce cyclic loads (e.g. by reducing the stiffness)
- Try to use other soil types for example a stiffer subsoil or a stiffer base material (e.g. a lightly bound material such as mixed granulate with “eloslakken”).
- Increase the wheel load to 50 kN again. Use different aggregate materials and/or apply an asphalt surface.
- Place the reinforcement a little bit higher in the base (say at 2/3 height of the base below the surface), the anchorage of the reinforcement should be better in that case. On the other hand the reinforcement will be transferred nearer towards the neutral axis.
- Investigate the influence of acceleration and braking forces of the vehicles.
- Validation of the calculations with e.g. a test pit.
- Investigate what the value of the bond is, by making use of the COI values for several aggregate materials. Estimate the D_{tt} values for reinforcement analyses.

References

1. Beers van P.J.J.M.: The strength and stiffness development of hydraulic mixed granulate. Faculty of Civil Engineering, Delft University of Technology, June 1998.

2. Bondt de A.H : Theoretical Analysis of Reinforced Pullout. Faculty of Civil Engineering, Delft University of Technology, December 1995.

3. Geotextiles in the roadconstruction and as road reinforcement. (in Dutch). CUR 175, Dutch geotextile organization, June 1991.

4. Houlsby & Jewell R.A.: Design of reinforced unpaved roads for small rut depths. Proceedings (volume 1) 4th international conference on geotextiles, geomembranes and related products, Balkema, Rotterdam, 1990.

5. Huang Y.H.: Pavement analysis and design. University of Kentucky, 1993.

6. Huurman M.: Permanent deformation in concrete block pavements. Ph.D. thesis, Delft University of Technology, December1997.

7. Jansma H.E.W., Sweere G.T.H.: Survey base materials test sites Schipluiden. (in Dutch). Faculty of Civil Engineering, Delft University of Technology, June 1988.

8. Liu X., Scarpas A.: Numerical Analyses of Road Performance with TRC-Grid. Faculty of Civil Engineering, Delft University of Technology, August 1997.

9. Maas K.: Survey in a pullout box regarding the friction behaviour in soil. (in Dutch). Faculty of Civil Engineering, Delft University of Technology, June 1994.

10. Molenaar A.A.A.: Stresses and strains in flexible pavements, Lecture notes, Faculty of Civil Engineering, Delft University of Technology, February 1993.

11. Molenaar A.A.A.: Structural Design of Pavements. Lecture notes, Faculty of Civil Engineering, Delft University of Technology, September 1994.

12. Scarpas A.: CAPA Finite Elements System, FEMA User's Manual. Faculty of Civil Engineering, Delft University of Technology, December 1994.

13. Sellmeijer J.B.: Design of geotextile reinforced paved roads and parking areas. Proceedings (volume 1) 4th international conference on geotextiles, geomembranes and related products, Balkema, Rotterdam, 1990.

14. Stet M.J.A., Sloten van G.G.: Designing light pavement structures. (in Dutch). KOAC Wegmeetdienst , Apeldoorn, August 1997.

15. Steward J., Mohney J.: Trail use results and experience using geotextiles for low volume forest roads. Proceedings (volume 2) Second international conference on geotextiles, Las Vegas, Nevada, USA, Industrial Fabrics Association International, 1982.